Table 1. Amino Acid Sequences of Synthetic Peptides Encompassing CC2 Used in the Study

Peptide	Residue	Sequence
P1	317–348	AEEDVWEILRQAPPSEYERIAFQYGVTDLRGM
P2	344–375	DLRGMLKRLKGMRRDEKKSTAFQKKLEPAYQV
P3	371–402	PAYQVSKGHKIRLTVELADHDAEVKWLKNGQE
P4	398–429	KNGQEIQMSGSKYIFESIGAKRTLTISQCSLA
P5	425–456	QCSLADDAAYQCVVGGEKCSTELFVKEPPVLI
P6	452–483	PPVLITRPLEDQLVMVGQRVEFECEVSEEGAQ
P7	479–510	EEGAQVKWLKDGVELTREETFKYRFKKDGQRH
P8	506–537	DGQRHHLIINEAMLEDAGHYALCTSGGQALRE
P9	533–564	QALRELIVQEKKLEVYQSIADLMVGAKDQAVF
P10	560–591	DQAVFKCEVSDENVRGVWLKNGKELVPDSRIK
P11	587–619	DSRIKVSHIGRVHKLTIDDVTPADEADYSFVPE
P12	615–647	SFVPEGFACNLSAKLHFMEVKIDFVPRQEPPKI

C-protein fragment 2 encompasses amino acid 317–647 residues of human cardiac C-protein.

findings, we performed transfer experiments and demonstrated that both activation of T cells and anti-peptide antibody elevation are required for the initiation and subsequent progression of the disease. The present study strongly suggests that B-cell epitope spreading is an essential step for the switch from myocarditis to DCM.

Materials and Methods

Animals and Proteins

Lewis rats were purchased from SLC Japan (Shizuoka) and bred in our animal facility. Seven- to 11-week-old male and female rats were used.

Preparation of Recombinant C-Protein Fragments and Synthetic Peptides

The preparation of recombinant C-protein was precisely described previously.[5] Polymerase chain reaction (PCR) products corresponding to fragments 1, 2, 3, and 4 were inserted into a cloning vector, pCR4 Blunt-TOPO in the Zero Blunt TOPO kit (Invitrogen, Groningen, The Netherlands), and clones with correct sequences were subcloned into an expression vector, pQE30 (Qiagen, Tokyo, Japan). Then, recombinant C-protein fragments produced in transformed *Escherichia coli* were isolated under denaturing conditions and purified using Ni-NTA Agarose (Qiagen).

Synthetic peptides encompassing CC2, designated as CC2P1-CC2P12 (Table 1), were synthesized using a peptide synthesizer (Shimadzu, Kyoto, Japan). All of the peptides used in this study were >90% pure as determined and were purified if necessary using HPLC.

Conjugation of CC2P12 with KLH

To increase immunogenicity of CC2P12, the peptide was conjugated with keyhole limpet hemocyanin (KLH; Wako, Tokyo, Japan) as described previously.[6] KLH (in 0.083 mol/L sodium phosphate, 0.9 mol/L NaCl, and 0.1 mol/L ethylenediamine tetraacetic acid, pH 7.2) and *m*-maleimidobenzoyl-*N*-hydrosuccinimide ester in dimethyl sulfoxide (MBS; Pierce, Chicago, IL) at concentrations of 10 and 20 mg/ml, respectively, were incubated at a ratio of 10:1 for 1 hour at room temperature. Then, excess MBS was removed on a HiTrap desalting column (Amersham Biosciences, Tokyo, Japan). Finally, the KLH-CC2P12 complex was formed by incubating MBS-KLH with CC2P12 for 2 hours at room temperature.

EAC Induction and Tissue Sampling

Lewis rats were immunized once on day 0 with the indicated antigen with complete Freund's adjuvant (CFA) (2.5 mg/ml *Mycobacterium tuberculosis*) in the hind foot pads. At the time of immunization, rats received an intraperitoneal injection of 2 μg of pertussis toxin (PT; Seikagaku Corp., Tokyo, Japan). The numbers of rats used for experiments are shown in the footnotes of tables and the figure legends. Histological and immunohistochemical examinations were performed at the indicated time points using frozen and paraffin-embedded sections of the heart. Although evaluation of EAC and DCM was mainly based on histological examinations (see below), clinical score was also recorded: grade 1, dyspnea; grade 2, dyspnea plus ruffling of fur; and grade 3, moribund condition or death.

Histological Grading of Inflammatory Lesions and Immunohistochemistry

EAC inflammatory lesions were evaluated using hematoxylin and eosin (H&E)-stained sections according to the following criteria: grade 1, rare focal inflammatory lesions; grade 2, multiple isolated foci of inflammation frequently associated with pericarditis; grade 3, diffuse inflammation involving the outer layer of the muscle; grade 4, grade 3 plus focal transmural inflammation; and grade 5; diffuse inflammation with necrosis. CC2 immunization induced pericarditis that was frequently associated with pericardial and pleural effusion. However, we did not include the findings in the scores because the above grading system covered the whole range of mild to severe EAC. The extent of fibrosis revealed by Azan staining was graded into five categories: grade 1, rare scattered foci of fibrosis; grade 2, multiple isolated foci of fibrosis; grade 3, fibrosis involving the outer layer of the

muscle; grade 4, grade 3 plus partial transmural fibrosis; and grade 5, diffuse fibrosis.

Establishment of T-Cell Lines and the Proliferative Assay

CC2- or CC2P12-specific T-cell lines were established from draining (popliteal) lymph node cells taken from CC2- or CC2P12-immunized rats by cycle stimulations with CC2 or CC2P12 in the presence of mitomycin C-treated thymocytes as antigen-presenting cells. Between antigen stimulations, T cells were propagated in culture medium containing 5% Con A supernatant.

Proliferative responses of lymph node cells were assayed in microtiter wells by the uptake of [^{3}H]thymidine. After being washed with phosphate-buffered saline, lymph node cells (2×10^5 cells/well) were cultured with the indicated concentrations of CC2 or CC2 peptides for 3 days, with the last 18 hours in the presence of 0.5 μCi of [^{3}H]thymidine (Amersham Pharmacia Biotech, Tokyo, Japan). In some experiments, the proliferative responses of CC2- or CC2P12-specific T-cell lines (3×10^4 cells/well) were assayed in the presence of the antigens and antigen-presenting cells (5×10^5 cells/well). The cells were harvested on glass-fiber filters, and the label uptake was determined using standard liquid scintillation techniques.

CDR3 Spectratyping

CDR3 spectratyping was performed as described previously.[7,8] In brief, PCR products were added to an equal volume of formamide/dye loading buffer and heated at 94°C for 2 minutes. The amplified PCR products were electrophoresed on polyacrylamide sequencing gels, and the fluorescence-labeled DNA profile on the gels was directly recorded using an FMBIO fluorescence image analyzer (Hitachi, Yokohama, Japan). The presence or absence of contaminations of the reagents used in PCR was examined every 10 PCR analyses by performing PCR without the templates. When contaminations were present, all reagents used and the results obtained during the period were discarded.

ELISA

The levels of anti-CC2 and anti-CC2 peptide antibodies were measured using the standard ELISA test. Recombinant CC2 and CC2P1-P12 (10 μg/ml) were coated onto microtiter plates, and serially diluted sera from normal and immunized animals were applied. After washing, appropriately diluted horseradish-conjugated anti-rat IgG, IgG1, or IgG2a was applied. The reaction products were then visualized after incubation with the substrate. The absorbance was read at 450 nm.

Generation of Polyclonal Antibodies Against CC2 and CC2 Peptides

Polyclonal antibodies against CC2 and CC2 peptides were raised by immunizing rats with the antigens/CFA four times on a weekly basis. Sera were obtained 1 week after the last immunization, and ammonium sulfate-precipitated preparations were used for the transfer experiments. The presence of antibodies against the indicated antigens was confirmed by ELISA.

Statistical Analysis

Unless otherwise indicated, Student's *t*-test or Mann-Whitney's *U*-test was used for the statistical analysis.

Results

Autoimmune Carditis-Inducing Ability of Recombinant C-Protein and Synthetic Peptides

As reported in our previous study,[5] recombinant CC2 (amino acid residues 317–647 of human cardiac C-protein) possessed the strongest carditogenic activity among four recombinant proteins encompassing the entire molecule. In the present study, we prepared 12 overlapping synthetic peptides (Table 1) covering the CC2 molecule and examined their carditis-inducing ability. As shown in Table 2, we first screened all of the peptides using the peptide mixtures (groups A through D). Only mixture 4 containing peptides 10, 11, and 12 at 100 μg of each peptide (CC2P10 to -P12) induced EAC in all of the immunized rats (group D), whereas mixtures 1, 2, and 3 induced mild EAC in one of three rats (groups A through C). Then, we tested the carditogenicity of each peptide in mixture 4 and found that only peptide 12 (CC2P12) possessed a carditis-inducing ability (group G). However, it should be noted that compared with CC2, both inflammation and fibrosis induced with CC2P12 were significantly milder as estimated on day 17 and 6 weeks after immunization (group G versus group I). Because immunization with 300 μg of CC2P12 did not differ to 100 μg of CC2P12 immunization in terms of the histological severity, the pooled data are shown in Table 2. In addition, CC2P12-immunized rats did not develop DCM at 6 weeks postimmunization (PI) (see below). Another important aspect was the survival rate. As shown in Figure 1, 75% of the rats immunized with CC2 died of cardiac failure by day 50 PI. In sharp contrast, all of the rats immunized with CC2P12 had survived by day 50. Furthermore, CC2P12 was conjugated with KLH to increase the immunogenicity, and rats were immunized with the conjugate. However, this procedure did not augment the carditis-inducing ability of CC2P12 (group H). In an additional experiment, we immunized rats with a mixture of P1, P5, P8, P11, and P12, but the histological score was not significantly different from that of P12-immunized rats (data not shown). Collectively, these findings suggest that substances induced after CC2P12 immunization lack

Table 2. Histological Severities of EAC Induced by Immunization with the Peptide Mixtures, Synthetic Peptides, and Recombinant CC2*

Group	Antigen	Sampling	Incidence	Inflammation	Fibrosis
A	Mix 1 (P1 to P3)	3 weeks	1/3	0.7 ± 0.7	0
B	Mix 2 (P4 to P6)	3 weeks	1/3	0.3 ± 0.3	0
C	Mix 3 (P7 to P9)	3 weeks	1/3	0.2 ± 0.2	0
D	Mix 4 (P10 to P12)	3 weeks	3/3	2.5 ± 1.2	0
E	P10	Day 17	0/3	0†	0
F	P11	Day 17	1/3	0.2 ± 0.2†	0
G	P12	Day 17	4/4	2.0 ± 0.4†	0
		6 weeks	6/6	1.8 ± 0.4†	1.8 ± 0.6‡
H	P12-KLH	4 weeks	2/3	0.7 ± 0.3	0.7 ± 0.3
		6 weeks	3/3	1.3 ± 0.3†	0.8 ± 0.4‡
I	CC2	Day 17	5/5	4.1 ± 0.4†	1.5 ± 0.4
		6 weeks	6/6	3.8 ± 0.2†	4.1 ± 0.2‡

*Lewis rats were immunized once with mixtures 1, 2, 3, and 4 that had consisted of peptides 1 to 3, 4 to 6, 7 to 9, and 10 to 12, respectively (100 μg of each peptide), in CFA in the foot pads along with intraperitoneal injection of pertussis toxin (2 μg). Because mix 4 showed carditogenicity, each peptide in the mixture (P10, P11, and P12) was tested in a similar manner. For comparison, the results obtained with recombinant C-protein fragment 2 are also shown. The denominators in the incidence column represent the number of rats used for each experiment.

†Analysis of variance and multiple comparison (Scheffe's F-test) were performed, and significant differences were noted in the following combinations: P10 versus CC2, $P = 0.002$; P11 versus CC2, $P = 0.0001$; P12 versus CC2, $P = 0.008$ on day 17; P12 versus CC2, $P = 0.003$; P12-KLH versus CC2, $P = 0.003$ at 6 weeks.

‡Significant differences were noted in the following combinations: P12 versus CC2, $P = 0.011$; P12-KLH versus CC2, $P = 0.004$ at 6 weeks.

some aggravation factors for EAC/DCM induced by immunization with CC2.

Figure 2 depicts normal histology of the heart (A, D, G, and J) and pathology of EAC induced by CC2 (B, E, H, and K) and CC2P12 (C, F, I, and L). At 2 weeks PI, when EAC was at the acute inflammatory stage, the hearts taken from CC2-immunized rats showed marked hypertrophy (Figure 1B), whereas the hearts from CC2P12-immunized rats showed slight enlargement (Figure 1C). We measured the long and short axes of the middle portion of normal, CC2-immunized, and CC2P12-immunized rats and calculated the heart area at this level. As shown in Table 3, there were significant differences between normal and CC2-immunized rats ($P = 0.01$) and between CC2- and CC2P12-immunized rats ($P = 0.005$), indicating that the hearts from CC2-immunized rats showed marked hypertrophy. In contrast, there was no significant difference between the normal and CC2P12-immunized groups. H&E (Figure 2, E and F) and azan (Figure 2, H and I) stainings showed that compared with CC2-induced EAC (Figure 2, E and H), both inflammation and fibrosis were mild (Figure 2, F and I). In sections immunostained for macrophages, there was extensive and diffuse macrophage infiltration in CC2-induced EAC (Figure 2K), whereas macrophage infiltration in CC2P12-induced EAC was mild and focal (Figure 2L). B-cell infiltration was absent in both types of EAC (data not shown).

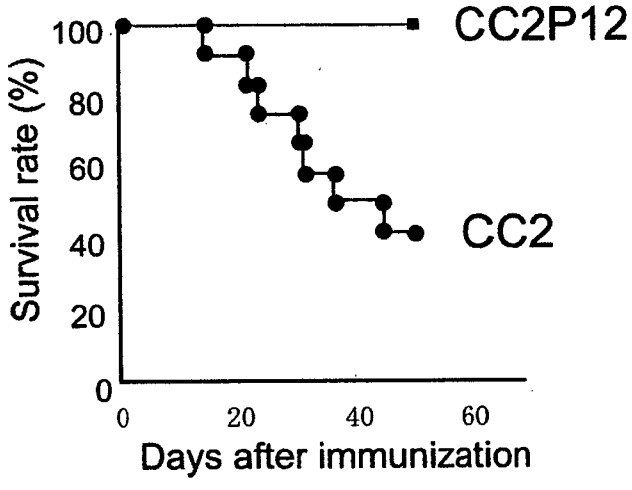

Figure 1. The survival rate of rats immunized with recombinant CC2/CFA or CC2P12/CFA with the intraperitoneal injection of pertussis toxin. Seventy-five percent of rats immunized with CC2 died between days 15 and 49 PI, whereas all of the rats immunized with CC2P12 survived during the observation period.

Characterization of Pathogenic T Cells

We next tried to determine whether a carditogenic peptide, CC2P12, contains an immunodominant or cryptic T-cell epitope. The representative results of three experiments are shown in Figure 3, A and B. When CC2 was immunized, the draining lymph node cells responded vigorously to CC2 but not to all of the overlapping peptide (P1 to P12 in Figure 3A). Similar experiments were performed using CC2-specific T-line cells after four to five cycles of antigen stimulation, and essentially the same results were obtained (data not shown). After CC2P12 immunization, lymph node cells responded well to CC2P12 and also to CC2 to a lesser extent (Figure 3B). These findings suggest that CC2P12 is processed and presented to T cells from CC2P12-immunized rats but is a cryptic epitope in the CC2 molecule for T cells from CC2-immunized rats.

In a previous study, we showed with CDR3 spectratyping analysis that in cardiac myosin-induced EAC, Vβ8.2 and Vβ10 TCR were clonally expanded in the inflamed heart and that Vβ8.2- and Vβ10-targeted immunotherapy was effective in ameliorating the severity of EAC.[7] We performed a similar analysis to characterize the nature of clonally expanded T cells in the heart with C-protein-induced EAC. The representative profiles are depicted in Figure 3, C and D, and all of the results are

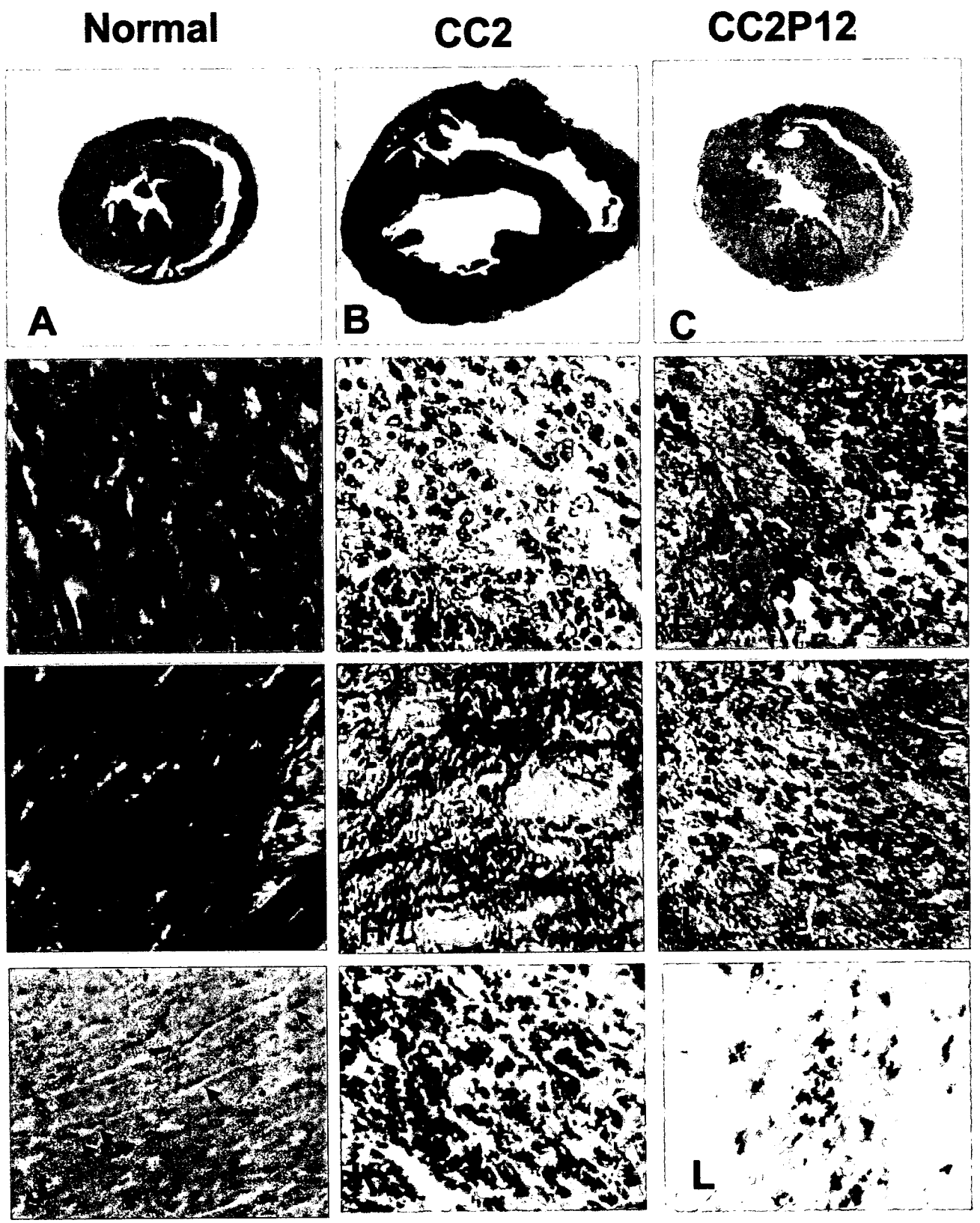

Figure 2. Normal histology (**A**, **D**, **G**, and **J**) and pathology of EAC induced by immunization with CC2 (**B**, **E**, **H**, and **K**) and CC2P12 (**C**, **F**, **I**, and **L**). At 2 weeks PI, when EAC was at the acute inflammatory stage, the hearts taken from CC2-immunized rats showed marked hypertrophy (**B**) compared with the normal heart (**A**), whereas the hearts from CC2P12-immunized rats showed only slight enlargement (**C**). H&E (**E** and **F**) and azan (**H** and **I**) stainings showed that compared with CC2-induced EAC (**E** and **H**), both inflammation and fibrosis of the heart were mild in CC2P12-immunized rats (**F** and **I**). In sections immunostained for macrophages, there was extensive and diffuse macrophage infiltration in CC2-induced EAC (**J**), whereas macrophage infiltration in CC2P12-induced EAC was mild and focal (**K**). **A–C:** H&E staining; the photographs were taken at the same magnification. **D–F:** H&E staining, ×240. **G–I:** Azan staining, ×240. **J–L:** ED1 staining, ×240.

Table 3. Measurements of Hearts under Normal and Diseased Conditions*

Condition	No. of rats examined	Diameter (mm)		Estimated area of hearts (mm^2)†
		Long axis	Short axis	
Normal	3	0.83 ± 0.10	0.72 ± 0.12	0.47 ± 0.14‡
CC2	6	1.20 ± 0.19	0.97 ± 0.08	0.91 ± 0.19‡
CC2P12	6	0.91 ± 0.08	0.80 ± 0.11	0.58 ± 0.13‡

*Rats were immunized once with CC2 or CC2P12, and the hearts were taken at 6 weeks after immunization. The long and short axes of the diameter were measured at the middle portion of the hearts. The hearts from CC2P12-immunized rats were measured before and after fixation, and those from normal and CC2-immunized rats were measured only after fixation. Because there was no significant change before and after fixation, all the values shown in the table are those measured after fixation.

†The heart area was calculated as long axis/2 × short axis × 3.14.

‡Significant differences were noted between normal and CC2-immunized rats ($P = 0.01$) and between CC2- and CC2P12-immunized rats ($P = 0.005$). However, there was no significant difference between normal and CC2P12-immunized rats.

summarized in Figure 3E. Infiltrating T cells in the heart of CC2-immunized rats on day 25 PI showed Vβ3 and Vβ4 expansion (Figure 3C, arrows), and those of CC2P12-immunized rats on day 17 PI showed Vβ4, Vβ8.6, and Vβ17 expansion (Figure 3D, arrows). The longitudinal study of CC2-immunized rats revealed interesting findings. On day 9 PI, T cells infiltrating the heart were rather heterogonous, and no particular Vβ expansion was noted (Figure 3E). In contrast, between days 14 and 28 PI when the inflammatory lesion reached at the maximal level,[5] Vβ4 expansion was detected in all of the cases examined. Other Vβs such as Vβ1, -7, -8.5, and -16 were expanded in one-half of the cases. Interestingly, T cells found in the heart at the later stage (6 and 10 weeks), when there was extensive fibrosis, showed the normal spectratype pattern (Figure 3E). These findings suggested that infiltrating T cells showing oligoclonal expansion play an important role in the development of EAC lesions (see the results of the transfer experiments below). However, T cells found at the later stage may be less involved in the disease progression. CDR3 spectratyping analysis of heart-infiltrating T cells of CC2P12-immunized rats was performed on day 17 and at 4 weeks PI and revealed that there was Vβ4 expansion in all of the cases examined. Taken together, Vβ4-positive T cells appear to play an important role in lesion formation in both CC2- and CC2P12-induced EAC, and there was no significant difference in the T-cell characteristics between the two groups.

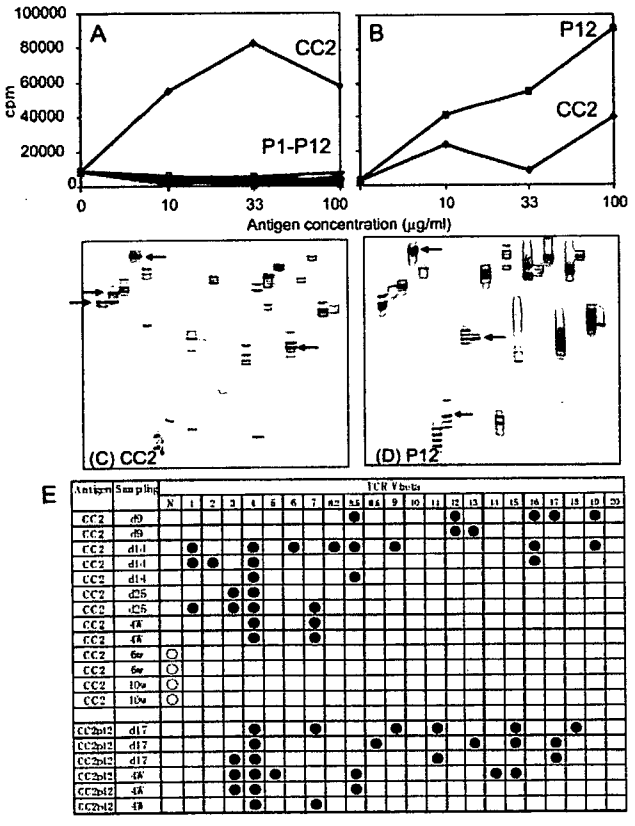

Figure 3. A and **B:** The proliferative responses of lymph node cells taken from CC2-immunized (**A**) and CC2P12-immunized (**B**) rats on day 12 PI. Lymph node cells (2×10^5 cells/well) were cultured with the indicated antigen for 72 hours, with the last 18 hours in the presence of [^{3}H]thymidine. The cells were harvested on glass-fiber filters, and the label uptake was determined using standard liquid scintillation techniques. Each symbol represents the mean value of triplicate assays, and SEMs were within 10% of the mean values. **C** and **D:** CDR3 spectratyping profiles of heart-infiltrating T cells taken from CC2-immunized (**C**) and CC2P12-immunized (**D**) rats. Marked spectratype expansions are indicated by **arrows**. **E:** Summary of the results of CDR3 spectratyping of T cells in the hearts from CC2- and CC2P12-immunized rats. Each line represents the result obtained from one rat. Closed circles represent Vβ clonal expansion. N, the normal spectratype pattern; w, weeks.

Characterization of Pathogenic B Cells and Anti-C-Protein Antibodies

As shown in Table 2 and Figure 2, CC2P12-immunized rats showed mild to moderate EAC without subsequent DCM. Moreover, unlike CC2-induced EAC, CC2P12-induced EAC was not fatal. These findings suggest that there are factors in CC2, but not in CC2P12, that aggravate EAC and induce DCM. Because we did not find clear differences between CC2- and P12-reactive T cells in the clonality analysis, we next examined the nature of antibodies raised by CC2 (Figure 4A) and CC2P12 (Figure 4B) immunization. From 1 to 12 weeks PI, sera were collected from CC2-immunized rats, and the levels of antibodies against CC2 and CC2P1 to -P12 were determined by ELISA (Figure 4A). At the early stage (1 to 3.5 weeks), only anti-CC2 antibodies were elevated in CC2-immunized rats. Then, anti-P8 and anti-P11 antibodies rose between 4 and 6 weeks, and some others showed at a high level thereafter. In one case examined at 12 weeks PI (4335 in Figure 4A), antibodies against all of the peptides were detected. This finding clearly showed that there was B-cell epitope spreading in CC2-immunized

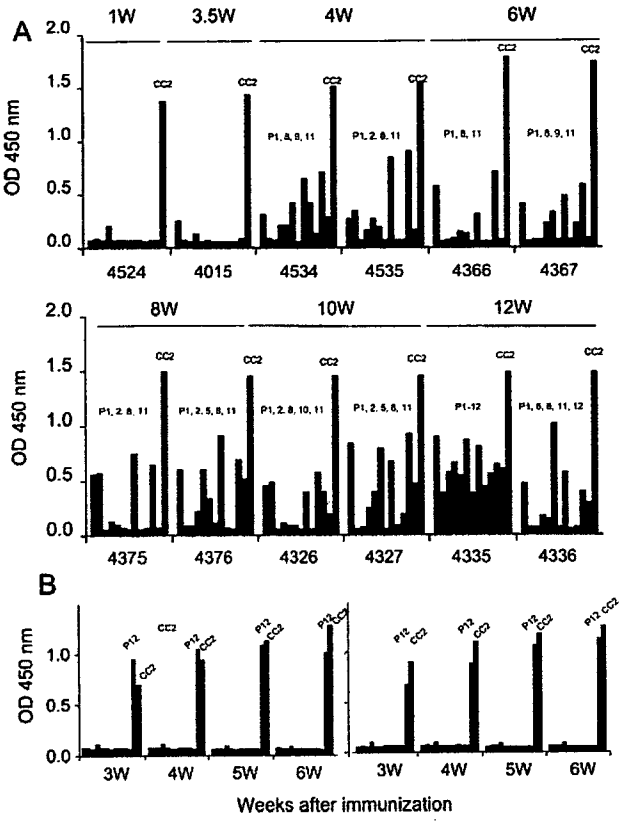

Figure 4. The kinetics of anti-CC2 and anti-CC2 peptide antibodies in CC2-immunized (**A**) and CC2P12-immunized (**B**) rats. **A:** The levels of anti-CC2 and anti-CC2 peptide antibodies were determined using ELISA. Recombinant CC2 and CC2P1-P12 (10 μg/ml) were coated onto microtiter plates, and diluted sera from CC2-immunized rats were applied. After washing, horseradish peroxidase-conjugated anti-rat IgG was allowed to react. The reaction products were then visualized after incubation with the substrate. The absorbance was read at 450 nm. **B:** The kinetics of anti-CC2 and anti-CC2 peptide antibodies in CC2P12-immunized rats. During the observation period, only anti-CC2P12 and anti-CC2 antibodies were elevated.

rats. Because this phenomenon was detected in the peripheral blood and there was no B-cell infiltration in the heart (data not shown), B-cell epitope spreading would take place in the lymphoid organ. In sharp contrast, in CC2P12-immunized rats, only antibodies against CC2P12 and CC2 were recognized in all of the rats examined by 6 weeks PI (Figure 4B).

CC2P12 Immunization and Cotransfer of Anti-CC2 or CC2 Peptide Antibodies Elicited Severe EAC

We further tried to identify factors that are responsible for the development of full-blown EAC and subsequent DCM. We already obtained the following findings. First, although CC2P12 was the sole carditis-inducing peptide in the CC2 molecule, CC2P12 induced relatively mild EAC without subsequent DCM. Second, there was no significant difference in the T-cell specificity between CC2-immunized and CC2P12-immunized rats. Finally, CC2-immunized rats showed marked intramolecular epitope spreading in the antibody production, whereas CC2P12-immunized rats developed antibodies that reacted with the immunizing antigen and the CC2 molecule. These findings raised the possibility that the generation of CC2-reacting T cells and generation of antibodies against various parts of the CC2 molecule are essential for full-blown EAC and subsequent DCM.

To test this possibility, we performed transfer experiments using various types of T cells and antibodies. The results are summarized in Table 4. Adoptive transfer of spleen and lymph node cells induced mild EAC in the recipients, whereas adoptive transfer of CC2-specific T-line cells did not elicit inflammation (Table 4, groups A and B). This finding suggests that not only T cells but also B cells are required for the development of inflammation in the heart. Cotransfer of anti-CC2 or anti-CC2P1–12 antisera after CC2P12 immunization aggravated both inflammation (Table 4, group D versus F, $P = 0.03$; group E versus F, $P = 0.005$) and fibrosis (Table 4, group D versus F, $P = 0.049$; group D versus F, $P = 0.01$) of EAC. There was no significant difference in the carditis-exacerbating ability between anti-CC2P1–12 and anti-CC2 antisera (Table 4, group D versus E). It should be noted that the transfer of anti-CC2 antisera alone did not induce EAC at all (group G). These findings strongly suggest that T cells are required for the initiation of inflammation in the heart and that anti-CC2 antibodies aggravate both inflammation and fibrosis.

Discussion

DCM is a serious problem for patients with heart failure because the disease progresses irreversibly and often ends in death. To develop effective therapies, it is essential to elucidate the pathomechanisms of the development of DCM. However, there are few good experimental models for DCM. In a previous study, we succeeded in inducing severe EAC with a high fatality rate and subsequent DCM in survivors by immunizing Lewis rats with cardiac C-protein.[5] This animal model is useful not only for the elucidation of the pathomechanisms of DCM but also for the development of effective immunotherapies.[5]

In the present study, we first tried to determine the carditis-inducing epitopes in the CC2 molecule and found that only peptide 12 (CC2P12), covering the residues 615–647, contains carditogenic epitope(s). Interestingly, immunization with CC2P12 induced moderate EAC but did not lead to subsequent DCM. Here, we demonstrated in a C-protein-induced animal model that B-cell epitope spreading occurred in CC2-immunized rats with DCM but not in CC2P12-immunized rats without DCM and that elevation of antibodies against various parts of the CC2 molecule is essential for the induction of more severe inflammation and fibrosis. However, it should be noted that activation of pathogenic T cells as demonstrated by CDR3 spectratyping is essential for the initiation of lesion formation because adoptive transfer of anti-CC2 antisera alone did not induce pathology at all.

Epitope spreading was first described in detail by Lehmann et al[9] as a key process for the development of chronic autoimmune encephalomyelitis. Initially, T-cell

Table 4. Summary of Cell and Antibody Transfer Experiments in EAC

Group	Immunization	Cell transfer		Ab transfer
		Cells	Dose	Ab
A	—	SpC + LNC*	10^7	—
B	—	CC2 TCL*	102 to 6 × 10^6	—
C	—	CC2P12 TCL*	3.5 to 6 × 10^6	—
D	CC2P12‡	—	—	Anti-P1-P12 sera
E	CC2P12‡	—	—	Anti-CC2 sera
F	CC2P12‡	—	—	Normal sera
G	—	—	—	Anti-CC2 sera

*CC2-reactive T cells or CC2P12 with or without antibodies were administered, and the degree of inflammation and fibrosis was evaluated 3 weeks after cell transfer. The denominators in the incidence column represent the number of rats used for each experiment. SpC, spleen cells; LNC, lymph node cells; TCL, T-cell line; —, not performed.

†n.e., not examined.

‡CC2P12 was immunized, and the indicated sera (1 ml after 5-fold dilution) were injected intravenously twice a week for 5 weeks. Rats were examined histologically 6 weeks after the immunization.

§Significant differences were noted in the following comparisons: D versus F, $P = 0.03$; E versus F, $P = 0.005$.

¶Significant differences were noted in the following comparisons: D versus F, $P = 0.049$; E versus F, $P = 0.01$.

(Table continues)

epitope spreading was intensively investigated, and this immunological event was thought to be highly involved in the relapse and chronicity of autoimmune diseases.[10–12] Later, it was reported that B-cell epitope spreading is also involved in the pathogenesis of autoimmune diseases.[13,14] Notably, Bischof et al[15] have shown that immunization of mice with myelin oligodendrocyte glycoprotein, but not with myelin basic protein and proteolipid protein, induced extensive B-cell epitope spreading and chronic autoimmune encephalomyelitis. Furthermore, they observed that diversification of the B-cell reactivity did not follow a sequential cascade that is seen in T-cell epitope spreading but represented a simultaneous spread toward a broad range of antigenic epitopes. In the present study, we also observed a similar mode of B-cell epitope spreading. Many reports have suggested that autoantibodies against cardiac components play an important role in the formation of DCM.[16–20] This assumption was also supported by the finding that immunoadsorption therapy to remove IgG ameliorated myocardial inflammation[4] and improved the cardiac performance and clinical status.[21] In addition, we have also observed that intravenous immunoglobulin administration suppressed the development of CC2-induced DCM and down-regulated anti-CC2 antibody production (our unpublished observation).

It is important to analyze the nature of DCM-inducing antibodies. We induced severe EAC with extensive fibrosis by immunization with CC2P12 plus transfer of anti-P1 to -P12 antisera that had been raised by peptide mixture immunization, but could not fully reconstitute the features of EAC and DCM produced by CC2 immunization. One of the reasons for this was that in our treatment protocol, it was difficult to maintain anti-peptide antibodies at a high level (unpublished observation). Although the reconstitution experiments demonstrated that anti-CC2P1–12 antisera possessed almost the same carditis-exacerbating ability as anti-CC2 antisera, there is a possibility that antibodies recognizing the conformational epitopes with high titers elicited by CC2 immunization but not by CC2P12 immunization are involved in the processes of DCM formation. In this regard, we are currently generating monoclonal antibodies against conformational epitopes of the CC2 molecule to test their ability of producing DCM. The conformational epitope mapping analysis would be helpful to identify pathogenic antibodies.

Increasing information about the pathogenesis of DCM will provide more chance for immunotherapies for the prevention and/or cessation of DCM. If pathogenic antibodies are identified more accurately, then specific and selective immunoadsorption could be achieved effectively with minimal side effects. In cases of DCM developed in a manner similar to that shown in the present study, intravenous immunoglobulin therapy, which is already in clinical trials,[22] is expected to be effective. Another important aspect is the timing of treatment initiation. As demonstrated in the previous[5] and present studies, histological examination revealed that fibrosis of the heart starts at 4 weeks PI and establishes at 6 to 8 weeks PI. Generation of the full range of pathogenic antibodies starts at the same period of time. Therefore, this time point is critical for the start of treatment. Improvements in the image analysis and functional studies are expected to greatly increase the effect of DCM therapy.

In summary, we identified the amino acid residue containing carditis-inducing epitope(s) in the CC2 molecule. By comparing CC2-induced EAC and subsequent DCM with peptide-induced EAC, it was demonstrated that B-cell epitope spreading is critical for the development of DCM. Importantly, by down-regulating pathogenic antibodies, it is possible to control the disease processes. Information obtained in the present study will provide useful information for the development of effective immunotherapies against human DCM.

Acknowledgment

We thank Y. Kawazoe for technical assistance.

Table 4. Continued

Ab transfer	Inflammation		Fibrosis	
Dose	Incidence	Grade	Incidence	Grade
—	2/2	2	n.e.†	n.e.
—	0/5	0	n.e.	n.e.
—	2/3	0.8 ± 0.6	0/3	0
5× dilution (1 ml) × 2/week × 5 weeks	3/3	3.3 ± 0.3§	3/3	3.3 ± 0.2¶
5× dilution (1 ml) × 2/week × 5 weeks	4/4	3.4 ± 0.3§	4/4	3.3 ± 0.3¶
5× dilution (1 ml) × 2/week × 5 weeks	4/4	1.5 ± 0.5§	4/4	1.6 ± 0.4¶
5× dilution (1 ml) × 2/week × 5 weeks	0/3	0	0/3	0

References

1. Liu PP, Mason JW: Advances in the understanding of myocarditis. Circulation 2001, 104:1076–1082
2. Parrillo JE, Cunnion RE, Epstein SE, Parker MM, Suffredini AF, Brenner M, Schaer GL, Palmeri ST, Cannon RO, Alling D, Wittes JT, Ferrnas VJ, Rodriguez ER, Fauci AS: A prospective, randomized, controlled trial of predonisone for dilated cardiomyopathy. N Engl J Med 1989, 321:1061–1068
3. Wojnicz R, Nowalany-Kozielska E, Wojciechowska C, Glanowska G, Wilczewski P, Niklewski T, Zembala M, Polonske L, Rozek MM, Wodniecki J: Randomized, placebo-controlled study for immunosuppressive treatment of inflammatory dilated cardiomyopathy. Circulation 2001, 104:39–45
4. Staudt A, Schaper F, Stangl V, Plagemann A, Bohm M, Merkel K, Wallukat G, Wernecke KD, Stangl K, Baumann G, Felix SB: Immunohistological changes in dilated cardiomyopathy induced by immunoadsorption therapy and subsequent immunoglobulin substitution. Circulation 2001, 103:2681–2686
5. Matsumoto Y, Tsukada Y, Miyakoshi A, Sakuma H, Kohyama K: C protein-induced myocarditis and subsequent dilated cardiomyopathy: rescue from death and prevention of dilated cardiomyopathy by chemokine receptor DNA therapy. J Immunol 2004, 173:3535–3541
6. Edwards RJ, Singleton AM, Boobis AR, Davies DS: Cross-reaction of antibodies to coupling groups used in the production of anti-peptide antibodies. J Immunol Methods 1989, 117:215–220
7. Matsumoto Y, Jee Y, Sugisaki M: Successful TCR-based immunotherapy for autoimmune myocarditis with DNA vaccines after rapid identification of pathogenic TCR. J Immunol 2000, 164:2248–2254
8. Kim G, Tanuma N, Kojima T, Kohyama K, Suzuki Y, Kawazoe Y, Matsumoto Y: CDR3 size spectratyping and sequencing of spectratype-derived T cell receptor of spinal cord T cells in autoimmune encephalomyelitis. J Immunol 1998, 160:509–513
9. Lehmann PV, Forsthuber T, Miller A, Sercarz EE: Spreading of T-cell autoimmunity to cryptic determinants of an autoantigen. Nature 1992, 358:155–157
10. McRae BL, Vanderlugt CL, Dal Canto MC, Miller SD: Functional evidence for epitope spreading in the relapsing pathology of experimental autoimmune encephalomyelitis. J Exp Med 1995, 182:75–85
11. Miller SD, Vanderlugt CL, Begolka WS, Pao W, Yauch RL, Neville KL, Katz-Levy Y, Carrizosa A, Kim BS: Persistent infection with Theiler's virus leads to CNS autoimmunity via epitope spreading. Nat Med 1997, 3:1133–1136
12. Vanderlugt CL, Neville KL, Nikcevich KM, Eagar TN, Bluestone JA, Miller SD: Pathologic role and temporal appearance of newly emerging autoepitopes in relapsing experimental autoimmune encephalomyelitis. J Immunol 2000, 164:670–678
13. Naserke HE, Ziegler AG, Lampasona V, Bonifacio E: Early development and spreading of autoantibodies to epitopes of IA-2 and their association with progression to type 1 diabetes. J Immunol 1998, 161:6963–6969
14. Li N, Aoki V, Hans-Filho G, Rivitti EA, Diaz LA: The role of intramolecular epitope spreading in the pathogenesis of endemic pemphigus foliaceus (fogo selvagem). J Exp Med 2003, 197:1501–1510
15. Bischof F, Bins A, Durr M, Zevering Y, Melms A, Kruisbeek AM: A structurally available encephalitogenic epitope of myelin oligodendrocyte glycoprotein specifically induces a diversified pathogenic autoimmune response. J Immunol 2004, 173:600–606
16. Warraich RS, Dunn MJ, Yacoub MH: Subclass specificity of autoantibodies against myosin in patients with idiopathic dilated cardiomyopathy: pro-inflammatory antibodies in DCM patients. Biochem Biophys Res Commun 1999, 259:255–261
17. Baba A, Yoshikawa T, Chino M, Murayama A, Mitani K, Nakagawa S, Fujii I, Shimada M, Akaishi M, Iwanaga S, Asakura Y, Fukuda K, Mitamura H, Ogawa S: Characterization of anti-myocardial autoantibodies in Japanese patients with dilated cardiomyopathy. Jpn Circ J 2001, 65:867–873
18. Caforio AL, Mahon NJ, Tona F, McKenna WJ: Circulating cardiac autoantibodies in dilated cardiomyopathy and myocarditis: pathogenetic and clinical significance. Eur J Heart Fail 2002, 4:411–417
19. Staudt A, Bohm M, Knebel F, Grosse Y, Bischoff C, Hummel A, Dahm JB, Borges A, Jochmann N, Wernecke KD, Wallukat G, Baumann G, Felix SB: Potential role of autoantibodies belonging to the immunoglobulin G-3 subclass in cardiac dysfunction among patients with dilated cardiomyopathy. Circulation 2002, 106:2448–2453
20. Staudt A, Staudt Y, Dorr M, Bohm M, Knebel F, Hummel A, Wunderle L, Tiburcy M, Wernecke KD, Baumann G, Felix SB: Potential role of humoral immunity in cardiac dysfunction of patients suffering from dilated cardiomyopathy. J Am Coll Cardiol 2004, 44:829–836
21. Müller J, Wallukat G, Dandel M, Bieda H, Brandes K, Spiegelsberger S, Nissen E, Kunze R, Hetzer R: Immunoglobulin adsorption in patients with idiopathic dilated cardiomyopathy. Circulation 2000, 101:385–391
22. Larsson L, Mobini R, Aukrust P, Gullestad L, Wallukat G, Waagstein F, Fu M: Beneficial effect on cardiac function by intravenous immunoglobulin treatment in patients with dilated cardiomyopathy is not due to neutralization of anti-receptor autoantibody. Autoimmunity 2004, 37:489–493

ARTHRITIS & RHEUMATISM
Vol. 56, No. 4, April 2007, pp 1304–1314
DOI 10.1002/art.22521

A New Murine Model to Define the Critical Pathologic and Therapeutic Mediators of Polymyositis

Takahiko Sugihara,[1] Chiyoko Sekine,[2] Takashi Nakae,[3] Kuniko Kohyama,[4] Masayoshi Harigai,[5] Yoichiro Iwakura,[6] Yoh Matsumoto,[4] Nobuyuki Miyasaka,[5] and Hitoshi Kohsaka[1]

Objective. **To establish a new murine model of polymyositis (PM) for the understanding of its pathologic mechanisms and the development of new treatment strategies.**

Methods. **C protein–induced myositis (CIM) was induced by a single immunization of recombinant human skeletal C protein in C57BL/6 mice, as well as in CD4-depleted, CD8-depleted, and mutant mice as controls. Some mice were treated with high-dose intravenous immunoglobulin (IVIG) after disease induction. Muscle tissues were examined histologically.**

Results. **In mice with CIM, inflammation was confined to the skeletal muscles. Histologic examination revealed a common pathologic feature of CIM and PM, involving abundant infiltration of CD8 and perforin-expressing cells in the endomysial site of the injured muscle. Suppression of myositis was achieved by depletion of both CD4 and CD8 T cells. Despite the development of serum anti–C protein antibodies in wild-type mice, severe myositis was induced in mice deficient in B cells. Induction of myositis was suppressed in interleukin-1α/β (IL-1α/β)–null mutant mice, but not in tumor necrosis factor α (TNFα)–null mutant mice. Use of IVIG, a treatment with proven efficacy in PM, suppressed CIM in the subgroup of treated mice.**

Conclusion. **CIM mimics PM pathologically and clinically. Infiltration of CD8 T cells is the most likely mechanism of muscle injury, and IL-1, but not B cells or TNFα, is crucial in the development of CIM. IVIG has therapeutic effects in CIM, suggesting that the effects of IVIG are not mediated by suppression of antibody-mediated tissue injury. This murine model provides a useful tool for understanding the pathologic mechanisms of PM and for developing new treatment strategies.**

Polymyositis (PM) is a chronic autoimmune inflammatory myopathy affecting striated muscles (1). Damage of muscles results in varying degrees of muscle weakness. Dysphagia with choking episodes and respiratory muscle weakness can occur in acute cases of PM. Currently, the pathogenesis of PM is unknown, and patients are therefore treated with nonspecific immunosuppressants. High-dose corticosteroids are the first-line treatment but are not effective in all patients. Improvement of disease often depends on the dosage of corticosteroids, making a dosage reduction difficult and thus, in many cases, necessitating administration of methotrexate or other immunosuppressants as adjunctive treatment. Because these medications can elicit a wide variety of adverse drug reactions, new therapies to address the specific pathologic features of PM are needed.

In affected muscles of patients with PM, infiltration of mononuclear cells leads to muscle fiber necrosis. These cells are found in the endomysial site, where non-necrotic muscle fibers are damaged, and also in the perimysial and perivascular sites of the muscles. Immunohistochemical studies have disclosed that CD8 T cells are most abundant in the endomysial site and invade

Supported by grants-in-aid from the Japanese Ministry of Education, Culture, Sports, Science, and Technology and from the Japanese Ministry of Health, Labor and Welfare.

[1]Takahiko Sugihara, MD, Hitoshi Kohsaka, MD, PhD: Tokyo Medical and Dental University, Tokyo, Japan, and Research Center for Allergy and Immunology, RIKEN, Yokohama, Japan; [2]Chiyoko Sekine, PhD: Research Center for Allergy and Immunology, RIKEN, Yokohama, Japan; [3]Takashi Nakae: Benesis Corporation, Osaka, Japan; [4]Kuniko Kohyama, MS, Yoh Matsumoto, MD, PhD: Tokyo Metropolitan Institute for Neuroscience, Tokyo, Japan; [5]Masayoshi Harigai, MD, PhD, Nobuyuki Miyasaka, MD, PhD: Tokyo Medical and Dental University, Tokyo, Japan; [6]Yoichiro Iwakura, DSc: University of Tokyo, Tokyo, Japan.

Address correspondence and reprint requests to Hitoshi Kohsaka, MD, PhD, Department of Medicine and Rheumatology, Graduate School, Tokyo Medical and Dental University, 1-5-45 Yushima, Bunkyo-ku, Tokyo 113-8519, Japan. E-mail: kohsaka.rheu@tmd.ac.jp.

Submitted for publication March 31, 2006; accepted in revised form January 16, 2007.

non-necrotic muscle fibers (2,3). These CD8 T cells express cytotoxic effector molecules, known as perforins, that are oriented toward target muscle fibers (4). Surface expression of class I major histocompatibility complex (MHC) molecules on muscle fibers is up-regulated (5). In a study of T cells from patients with PM compared with normal donors, CD8 T cell clones expanded more frequently in the peripheral blood of patients with PM (6,7). Moreover, some of these clones could be found in muscle biopsy samples from the same patients (6,7). All of these observations support the view that PM is driven by cytotoxic CD8 T cells.

In rheumatoid arthritis (RA), another autoimmune disease, biologic agents that block tumor necrosis factor α (TNFα) have been introduced into clinical use. TNFα blockade has an enormous effect in modulating the clinical course of RA (8). Animal models of arthritis serve to help identify therapeutic targets and to test the effect of these therapeutic reagents (9–11). In contrast, in PM, the lack of appropriate animal models has hampered basic research studies and delayed the development of new treatments.

Experimental autoimmune myositis (EAM), established previously as an animal model of PM, is inducible specifically in SJL/J mice by repeated administration of muscle homogenate or partially purified myosin (12,13). This model is a complex representation of disease, because SJL/J mice have a dysferlin gene mutation that causes spontaneous muscle necrosis and secondary muscle inflammation (14). Immunohistochemical studies have shown that infiltrating T cells in the muscle are dominated by CD4 T cells, suggesting that the EAM disease model is mediated by CD4 T cells (15).

We established a new murine model that can be induced with a single injection of a recombinant skeletal muscle fast-type C protein. This myosin-binding protein is in the cross-bridge–bearing zone of A bands of myofibrils (16,17). Biochemical purification studies showed that C protein appears to be the main immunopathogenic component of the crude skeletal-muscle myosin preparation used for the induction of experimental myositis in Lewis rats (18,19). In this study, we used recombinant protein fragments to confirm the immunogenicity of the C protein. This myositis, designated as C protein–induced myositis (CIM), can be induced in C57BL/6 (B6) mice and in other strains of mice. Its histologic and immunohistochemical features mimic those of PM. Functional studies have indicated that cytotoxic CD8 T cells are primarily responsible for the pathologic mechanisms of this disease.

Susceptibility to CIM in B6 mice has facilitated studies of the immunologic components required to induce myositis. In the present study, we were able to show that the effects of immunoglobulins are not necessary for the development of CIM, despite the presence of B cells in the affected muscles and anti–C protein antibodies in the sera. Although both interleukin-1 (IL-1)–positive and TNFα-positive cells infiltrated the muscles of affected mice, only IL-1, not TNFα, was crucial in the development of CIM. Interestingly, CIM was suppressed by infusion of intravenous immunoglobulins (IVIGs), which has been used as a last resort for treatment of patients with PM who do not respond to or tolerate immunosuppressive reagents. Thus, we show that our new model is useful in investigating the pathologic mechanisms of autoimmune myositis and in developing new treatment strategies for this disease.

MATERIALS AND METHODS

Mice. B6, SJL/J, BALB/c, DBA/1, and C3H/He mice were purchased from Charles River (Yokohama, Japan). NZB and MRL/Mp+/+ mice were purchased from SLC (Shizuoka, Japan). Mutant B6 mice rendered double-null for IL-1α/β were established previously (20), while Igμ-null mutant B6 mice (21) and TNFα-null mutant mice (22) were kindly provided by Drs. Karasuyama (Tokyo Medical and Dental University) and Sekikawa (formerly at the National Institute of Agrobiological Science), respectively. All experiments were done under specific pathogen–free conditions in accordance with the ethics and safety guidelines for animal experiments of Tokyo Medical and Dental University and RIKEN.

Recombinant human skeletal C protein. Four complementary DNA (cDNA) fragments encoding overlapping cDNA fragments 1, 2, 3, and 4 of human fast-type skeletal muscle C protein were amplified from human skeletal muscle cDNA using polymerase chain reaction. Primers used were 5′-GAGAGGTACCATGCCTGAGGCAAAACCAGCG-3′ and 5′-GAGAGTCGACTCAGAACCACTTGAGGGTCAGGTC-3′ for fragment 1, 5′-GAGAGGATCCGACCTGACCCTCAAGTGGTTC-3′ and 5′-GAGAAAGCTTTCACAGCCAGGTAGCGACGGGAGG-3′ for fragment 2, 5′-AGAGGATCCCCTCCCGTCGCTACCTGGCTG-3′ and 5′-GAGAAAGCTTTCACCGGGGCTTTCCCTGGAAGGG-3′ for fragment 3, and 5′-AGAGGATCCCCCTTCAGGGAAAGCCCCGG-3′ and 5′-GAGAAAGCTTTCACTGCGGCACTCGGACCTC-3′ for fragment 4 (Qiagen, Hilden, Germany) (underlining indicates the restriction enzyme recognition sites for subcloning into the pQE30 expression vector). These primers were introduced into the TOP10F′ bacterial host (Invitrogen, Carlsbad, CA) and were used to prepare recombinant C protein fragments according to the manufacturer's protocol. Soluble recombinant C proteins were dialyzed against 0.5*M* arginine, 2 m*M* reduced glutathione, 0.2 m*M* oxydized glutathione in phosphate buffered saline (PBS), pH 7.4 (fragments 1 and 2) or 25 m*M* glycine HCl, pH 3.0

(fragments 3 and 4). Endotoxin was removed using Detoxi-Gel Endotoxin Removal Gel (Pierce, Rockford, IL).

Induction of CIM. Female mice, ages 8–10 weeks, were immunized intradermally with 200 μg of the C protein fragments emulsified in Freund's complete adjuvant (CFA) containing 100 μg of heat-killed *Mycobacterium butyricum* (Difco, Detroit, MI). The immunogens were injected at multiple sites of the back and foot pads, and 2 μg of pertussis toxin (PT) (Seikagaku Kogyo, Tokyo, Japan) in PBS was injected intraperitoneally at the same time. Hematoxylin and eosin–stained 10-μm sections of the proximal muscles (hamstrings and quadriceps) were examined histologically for the presence of mononuclear cell infiltration and necrosis of muscle fibers. The histologic severity of inflammation in each muscle block was graded as follows (18,19): grade 1 = involvement of a single muscle fiber or <5 muscle fibers; grade 2 = a lesion involving 5–30 muscle fibers; grade 3 = a lesion involving a muscle fasciculus; and grade 4 = diffuse, extensive lesions. When multiple lesions with the same grade were found in a single muscle block, 0.5 point was added to the grade.

Immunohistochemical analysis. Cryostat-frozen sections (6 μm) fixed in cold acetone were stained with anti-CD8a (53-6.7; BD Biosciences PharMingen, San Diego, CA), anti-CD4 (H129.19; BD Biosciences PharMingen), anti-B220 (RA3-6B2; BD Biosciences PharMingen), anti-CD11b (M1/70; BD Biosciences PharMingen), anti-CD68 (FA-11; Serotec, Oxford, UK), anti–IL-1α (40508; Genzyme/Techne, Minneapolis, MN), or anti-TNFα (MP6-XT22; BioLegend, San Diego, CA) monoclonal antibodies (mAb). To stain perforin molecules, air-dried sections were treated with 0.5% periodic acid solution and then stained with antiperforin mAb (CB5.4; Alexis Biochemicals, San Diego, CA). Nonspecific staining was blocked with 4% Blockace (Dainippon, Osaka, Japan).

Bound antibodies were visualized with peroxidase-labeled anti-rat IgG antibodies and associated substrates (Histofine Simple Stain Max PO; Nichirei, Tokyo, Japan). The sections were also stained with biotinylated mouse anti-mouse H-2K^b mAb (AF6-88.5; BD Biosciences PharMingen) and with biotinylated mouse anti-mouse I-A^b mAb (AF6-120.1; BD Biosciences PharMingen). They were then incubated with peroxidase-conjugated streptavidin and its substrates (Chemicon, Temecula, CA). For double immunofluorescence staining, the sections were preincubated with 5% heat-inactivated rat serum and 1% bovine serum albumin, and were stained with Alexa Fluor 647–conjugated anti-CD8a mAb (53-6.7; BD Biosciences PharMingen) and fluorescein isothiocyanate (FITC)–conjugated anti-CD4 mAb (RM4-5; BD Biosciences PharMingen).

The bound antibodies were visualized using SP2AOBS confocal laser microscopy (Leica, Heidelberg, Germany). Spleens or popliteal lymph nodes were stained as positive controls. Isotype controls were used as negative control. The stained sections were evaluated by 2 independent observers, who reported results that were comparable.

Quantification of mononuclear cell subsets. The method used to quantify stained cells in the immunohistochemical analysis was based on a previously published method (2). Briefly, 5 inflammatory mononuclear cell foci in the serial sections from 4 mice with CIM were studied. At least 1 focus from each mouse was evaluated. Stained mononuclear cells infiltrating into the endomysial, perimysial, and perivascular sites of the foci were enumerated separately. The frequency of each subset was calculated in relation to the sum of all subsets. The CD4:CD8 ratios were calculated on the basis of these calculations. The CD4:CD8 ratios in double immunofluorescence staining were calculated in the same manner as in the immunohistochemical analyses. CD68-positive and CD11b-positive cells in the serial sections were also enumerated in the same manner, and the frequencies of CD68-positive cells were calculated in relation to the number of CD11b-positive cells.

Rotarod test. Muscle function was evaluated with a MK-630 rotarod device (Muromachi Kikai, Tokyo, Japan) as described previously (23). The rotarod test was performed on each mouse by measuring the running time until the mouse fell off the rod while the rod was turning at 20 revolutions per minute for 200 seconds. The running ability of each mouse was scored in 5 categories of running time: score 1 = 0–49 seconds, score 2 = 50–99 seconds, score 3 = 100–149 seconds, score 4 = 150–200 seconds, score 5 = >200 seconds. Mice were initially trained to accommodate them to the task, and then tested 2 days thereafter.

In vivo depletion of CD8 or CD4 T cells. For the depletion of CD8 or CD4 T cells in B6 mice, the mice were injected intraperitoneally with 1 mg of purified anti-CD8 (53.67.2) mAb (24), anti-CD4 (GK1.5) mAb (24), or purified rat IgG (Sigma-Aldrich, St. Louis, MO) as a control, for 3 consecutive days. This treatment started 10 days before the immunization. Injection of 500 μg of the same mAb was repeated every other day for 14 days. Splenocytes and lymph node cells from the treated mice were stained with phycoerythrin (PE)–conjugated anti-CD8 mAb (53.67; BD Biosciences PharMingen) or PE-conjugated anti-CD4 mAb (H129.19; BD Biosciences PharMingen), together with FITC-conjugated anti-CD3 mAb (145-2C11; BD Biosciences PharMingen). The cells were then analyzed with FACSCalibur (Becton Dickinson, San Jose, CA).

IVIG treatment. A subgroup of the mice were treated with IVIG. Human gamma immunoglobulins (Venoglobulin-IH; Benesis, Osaka, Japan) (400 mg/kg/day) were injected intravenously into the tail vein for 5 consecutive days, beginning 3 days after immunization.

Statistical analysis. Histologic scores were compared with the Mann-Whitney U test. *P* values less than or equal to 0.05 were considered significant.

RESULTS

Histologic features of CIM in immunized mice. Recombinant human fast-type skeletal C protein fragments were prepared using a prokaryotic expression system. Because of the size of the C protein, 4 overlapping protein fragments were generated: fragment 1 (amino acids 1–290), fragment 2 (amino acids 284–580), fragment 3 (amino acids 567–877), and fragment 4 (amino acids 864–1142). B6 mice were immunized at multiple sites of the back and foot pads with each fragment emulsified in CFA. PT was also injected intraperitoneally. To compare the immunogenicity of the 4 fragments, 5 mice per group were immunized with each

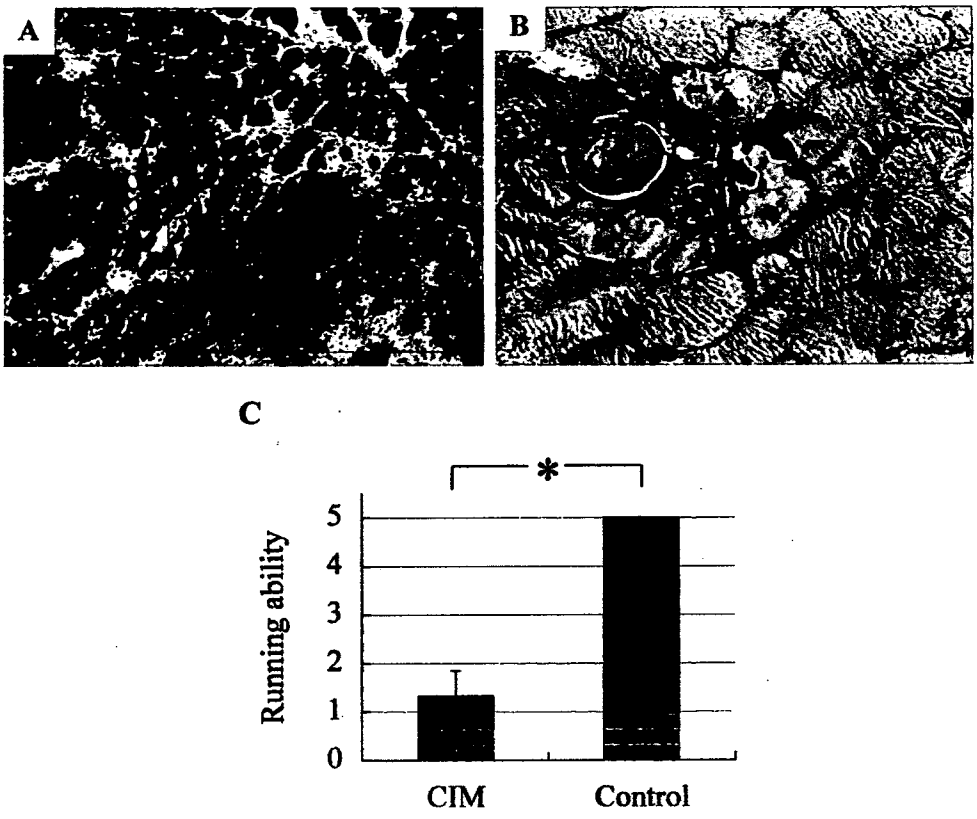

Figure 1. Muscle inflammation in C protein–induced myositis (CIM). C57BL/6 mice were immunized once with recombinant human skeletal C protein fragment 2 to induce CIM. **A** and **B**, Mononuclear cell infiltration was found predominantly in the endomysial site (boxed area) but also in the perimysial site (**solid arrows**) and perivascular site (**open arrows**) (**A**). Many cells invaded non-necrotic muscle fibers (**arrows**), while necrotic fibers were also present (**B**). Bar in **A** = 100 μm; bar in **B** = 25 μm. **C**, Muscle function was evaluated with a rotarod test 21 days after immunization. Six mice with CIM and 5 control mice treated with adjuvant alone were examined. Running ability was scored as described in Materials and Methods. Values are the mean and SD score. * = $P < 0.01$.

fragment, and myositis was studied histologically 21 days after the immunizaton.

None of the mice treated with adjuvant alone or immunized without PT developed myositis. We found that a single immunization of fragments 2 or 4 induced myositis consistently, and the mean ± SD histologic scores were 2.8 ± 0.2 and 1.0 ± 0.3, respectively. Fragments 1 and 3 induced milder myositis at a lower incidence, and the mean ± SD histologic scores were 0.2 ± 0.3 and 0.1 ± 0.2, respectively. Because fragment 2 induced the most severe myositis, it was used as an immunogen in subsequent experiments.

Histologic analysis of the muscles affected by CIM showed that mononuclear cells infiltrated predominantly the endomysial site, but also the perimysial and perivascular sites of the muscle tissue (Figure 1A). Many mononuclear cells invaded non-necrotic muscle fibers (Figure 1B). No abnormality in cardiac muscle and other tissues, including lung and joint tissues, was observed. Muscle function was assessed clinically with a rotarod device on day 21. Consistent with the histologic findings in the muscle tissue, mice with CIM ran for a shorter time than did control mice, indicating a reduction in motor function (Figure 1C).

Inflammation is acute and regresses spontaneously in most animal models of autoimmune diseases. To study the course of CIM in mice, muscle sections from 4 or 5 mice were examined at various time points after the immunization. A small number of mononuclear cells appeared in 50% of the muscle samples on day 7

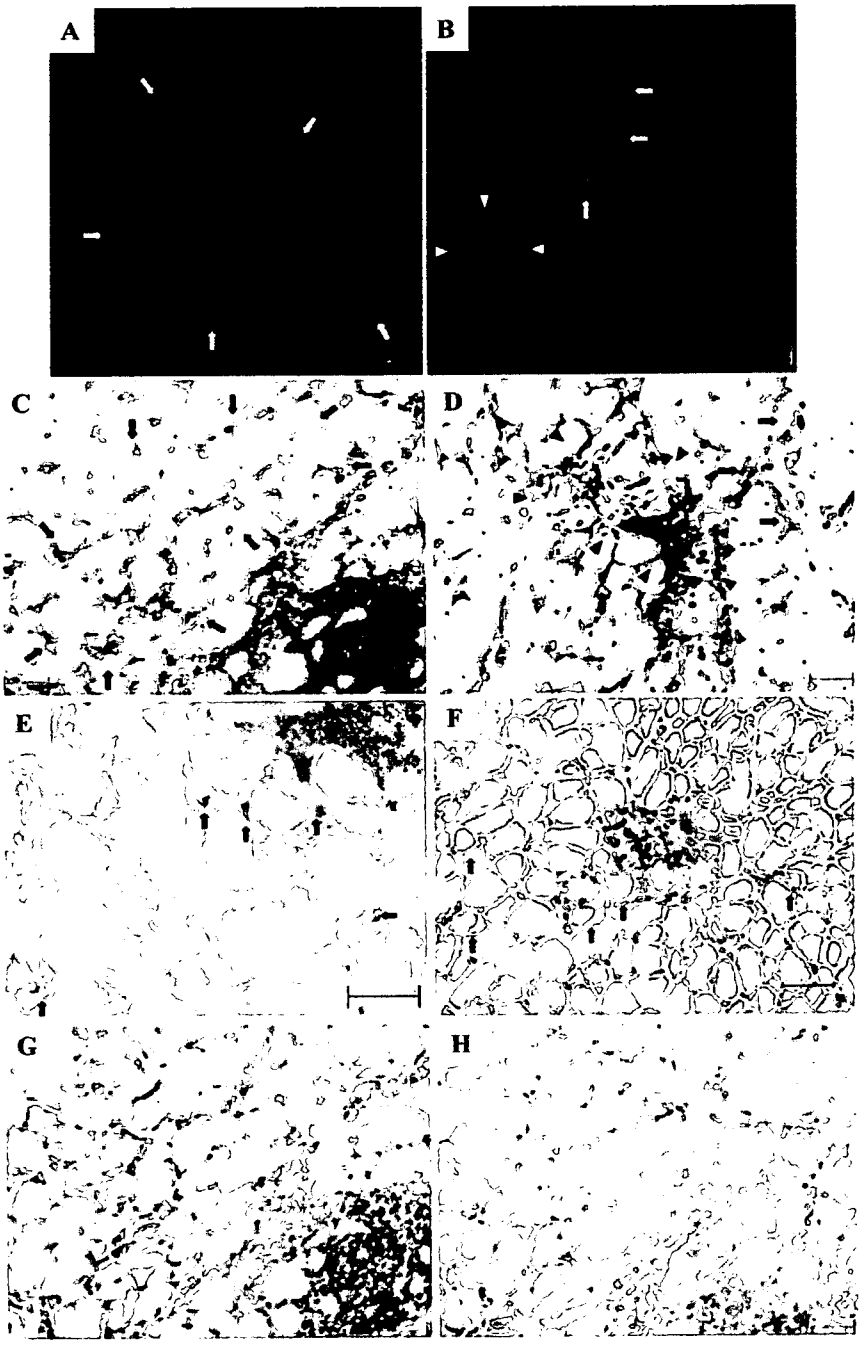

Figure 2. Immunohistochemical findings in muscles of mice with C protein–induced myositis. **A** and **B**, Expression of CD4 (green, fluorescein isothiocyanate) and CD8 (red, Alexa Fluor 647) was examined. Infiltrating cells in the endomysial site (**arrows**) (**A**) and in the perimysial site (**arrows**) and perivascular site (**arrowheads**) (**B**) were individually enumerated for calculating CD4:CD8 ratios. **C–H**, Expression of CD11b (**C** and **D**), perforin (**E**), class I major histocompatibility complex (**F**), interleukin-1α (IL-1α) (**G**), and tumor necrosis factor α (TNFα) (**H**) was examined with immunoperoxidase staining. CD11b-positive cells diffusely infiltrated the endomysial site (**arrows**) (**C**) and both the perimysial (**arrows**) and perivascular sites (**arrowheads**) (**D**). Perforin-positive cells infiltrated around non-necrotic muscle fibers at the endomysial sites (**arrows**) (**E**). Muscle fibers reacted to anti-H2K^b monoclonal antibodies (**arrows**) (**F**). IL-1α and TNFα were expressed on infiltrating mononuclear cells in muscles (**G** and **H**). Bars = 50 μm.

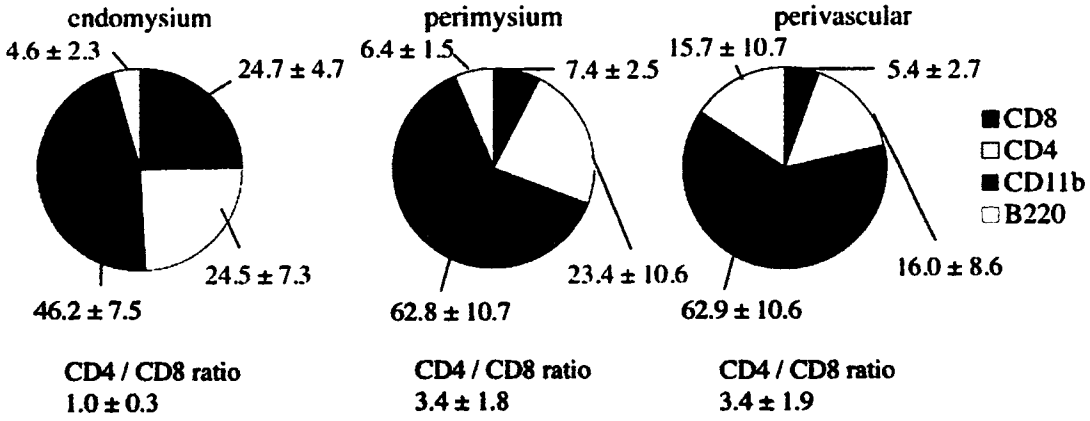

Figure 3. Quantitative immunohistochemical analysis of mononuclear cells in muscles of mice with C protein–induced myositis. Frequencies of CD8, CD4, CD11b, and B220 cells in the infiltrating mononuclear cells at endomysial, perimysial, and perivascular sites are shown. Values are the mean ± SD percentage of each cell subset and mean ± SD CD4:CD8 ratio at 5 inflammatory mononuclear cell foci. The total mononuclear cell counts in the endomysial, perimysial, and perivascular sites were 1,385, 506, and 543, respectively.

(incidence 50%, mean ± SD histologic score 0.6 ± 0.7). Inflammation of the muscle tissue peaked on days 14 and 21 after the immunization (incidence 100%, histologic scores 2.6 ± 0.3 and 2.8 ± 0.2, respectively) and started to resolve after day 28 (incidence 100%, histologic score 1.4 ± 0.6). On day 49, mononuclear cell infiltration was absent from most skeletal muscles. On days 35, 49, and 63, the histologic scores were 0.5 ± 0.6, 0.1 ± 0.2, and 0.0 ± 0.0, respectively, and the incidences of CIM were 38%, 10%, and 0%, respectively.

Other strains of mice were immunized with fragment 2 of the C protein in the same manner as in B6 mice, and the muscles were examined histologically. Studies of 4 or 5 mice per strain showed that myositis developed in NZB and SJL/J mice with an incidence similar to that in B6 mice. However, the mononuclear cell infiltration was less intense. The mean ± SD histologic scores were 1.8 ± 0.6 and 1.3 ± 0.3 in NZB and SJL/J mice, respectively. No inflammation was observed in the muscles from BALB/c, DBA/1, C3H/He, or MRL/Mp+/+ mice immunized with C protein fragments.

Immunohistochemical findings in muscles of mice with CIM. Localization of CD4 and CD8 T cells was studied with double immnunofluorescence labeling or immunohistochemical staining of muscle sections. CD4 cells diffusely infiltrated the endomysial, perimysial, and perivascular sites. In contrast, CD8 cells infiltrated preferentially the endomysial site (Figures 2A and B), which was reflected equally well in the CD4:CD8 cell ratios. Double immnunofluorescence staining of CD4 and CD8 cells showed that the mean ± SD CD4:CD8 ratios in the endomysium, perimysium, and perivascular site were 1.0 ± 0.1, 3.3 ± 0.3, and 3.5 ± 0.4, respectively, which was consistent with the ratios derived from immunohistochemical staining (Figure 3). The frequency of CD8-positive cells in endomysial sites was higher than that in perimysial and perivascular sites, whereas the frequencies of CD4-positive T cells were similar among the 3 sites (Figure 3).

B cells and macrophages were identified by staining with B220 and CD11b antibodies, respectively. CD11b-positive cells were most abundant among the infiltrating cells in all 3 sites (Figures 2C and D and Figure 3). Although natural killer cells are also CD11b positive, our analysis of CD68 and CD11b expression in serial sections showed that 93.4 ± 4.3% (mean ± SD) of CD11b-positive cells were CD68-positive cells, indicating that the majority of CD11b-positive cells were macrophages.

B cells were sparse in the muscle tissue, especially in the endomysial and perimysial sites (Figure 3). Perforin-positive cells were present mostly (82%) around non-necrotic muscle fibers at the endomysial site (Figure 2E) and were sparse in the perimysial and perivascular sites (results not shown). Thus, the distribution of perforin-positive cells corresponded well to that of CD8-positive cells. When muscle fibers were stained with anti-H2K^b (class I MHC) and anti-I-A^b (class II MHC) mAb, they reacted to the anti–class I

MHC mAb (Figure 2F) but not to the anti–class II MHC mAb (results not shown).

Pathologic role of CD8 and CD4 T cells in CIM. Histologic studies have demonstrated that CD8 T cells function as effector cells in injury of muscle fibers. To establish the pathologic role of CD8 T cells, B6 mice were pretreated by removal of circulating CD8 T cells using specific mAb. Ten days after injection of the antibodies for 3 consecutive days, CD8 T cells in the spleens were depleted to fewer than 2%. The mice were then immunized with C protein and treated with the same antibodies every other day for 14 days. The muscles were examined histologically 14 days after the immunization, when the frequency of CD8 T cells in the spleens and lymph nodes was still less than 2%. The number of CD4 T cells in the spleens and lymph nodes was maintained in the CD8-depleted mice.

Significantly fewer CD8-depleted mice developed myositis compared with control mice, with a 33% incidence of disease compared with 100% in controls (Table 1). The histologic scores of the treated mice were significantly lower than that of the controls. It is known that CD4 T cells help CD8 T cells develop into mature cytotoxic T lymphocytes. They also have the potential to injure muscle fibers. Therefore, CD4 T cells were removed with specific mAb in the same manner as described above for CD8 T cells. The pretreated mice exhibited fewer than 2% of circulating CD4 T cells, and were then immunized for CIM induction. They also developed a milder myositis compared with control mice (Table 1).

Investigation of essential immunologic mediators in mutant mice. Mice with CIM developed serum antibodies directed to C protein. They also developed low-titer autoantibodies with a cytoplasmic pattern or homogeneous and speckled nuclear patterns on Hep-2 staining, which proved to be nonreactive to PM-associated autoantigens (results not shown). However, the contribution of these autoantibodies to myositis was unclear.

The susceptibility of B6 mice to CIM allowed us to study the contribution of different immune mediators to myositis using genetic mutant mice. Igμ-null mutant mice developed CIM with features and a frequency comparable with those in control wild-type (WT) mice (Table 1). These findings indicate that the functions of B cells and immunoglobulins are not necessary for the development of CIM.

Inflammatory cytokines such as IL-1 and TNFα are known to be expressed in mononuclear cells infiltrating the muscles of mice with PM (25,26). Our immunohistochemical analyses showed that these inflammatory cytokines were also found in mice with CIM (Figures 2G and H). We then studied whether the presence of IL-1 and TNFα is required for the development of CIM, using IL-1α/β double-null mutant and TNFα-null mutant B6 mice. Most IL-1α/β–null mutant mice did not develop myositis, and those that did have myositis developed a mild form (Table 1). The rotarod score of 7 for the IL-1α/β–null mutant mice was significantly higher than that for the 6 WT mice (mean ± SD score 4.7 ± 0.5 versus 1.3 ± 0.5; $P < 0.01$). In contrast, TNFα-null mutant mice were as susceptible to CIM as the control mice, and the TNFα-null mice had a similar incidence and severity of myositis (Table 1). These results indicate the differential requirements for the roles of IL-1 and TNFα in the development of CIM.

Table 1. Studies of the pathologic features of C protein–induced polymyositis (CIM) and effects of treatment with intravenous immunoglobulin (IVIG)*

Experiment, mouse group	Incidence of CIM, %	Muscle blocks involved, %†	Histologic score, mean ± SD
CD8 depletion			
CD8-depleted	33	25	0.6 ± 1.0‡
Rat IgG–injected	100	100	1.9 ± 0.6
CD4 depletion			
CD4-depleted	60	50	0.7 ± 0.7‡
Rat IgG–injected	100	100	2.0 ± 0.4
Igμ-null			
Ig$\mu^{-/-}$	100	95	1.7 ± 0.6
WT	100	100	2.1 ± 0.7
IL-1-null			
IL-1$\alpha/\beta^{-/-}$	14	7	0.1 ± 0.2§
WT	100	100	2.1 ± 0.5
TNFα-null			
TNF$\alpha^{-/-}$	80	80	1.9 ± 1.0
WT	100	90	2.3 ± 0.6
IVIG			
IVIG-injected	43	36	0.6 ± 1.1‡
Saline-injected	100	100	2.3 ± 1.0

* Mice were immunized with 200 μg of the recombinant C protein fragments and then examined histologically 14 or 21 days after immunization. For in vivo depletion of CD8 or CD4 T cells, 5 or 6 B6 mice were treated intraperitoneally with anti-CD8 or anti-CD4 monoclonal antibodies, while 5 or 6 control mice were treated with purified rat IgG. To demonstrate the requirement for humoral immunity, the presence of interleukin-1 (IL-1), and the presence of tumor necrosis factor α (TNFα) for the development of CIM, 5 Igμ-null mutant mice, 7 IL-1α/β–null mutant mice, 5 TNFα-null mutant mice, and 5 wild-type (WT) B6 mice were studied. IVIG was administered at a dosage of 400 mg/kg/day intravenously into the tail vein for 5 consecutive days, from day 3 after immunization. Seven mice were treated with IVIG and 6 with control saline.

† Calculated as the number of muscle blocks showing myositis divided by the total number of blocks.

‡ $P < 0.05$ versus control group.

§ $P < 0.01$ versus control group.

Effects of high-dose IVIG treatment. Infusion of high-dose IVIG is effective treatment of inflammatory myopathies that are refractory to conventional immunosuppressants (27–29). Although several mechanisms of action for IVIG have been proposed, they have not been fully characterized. One possibility is that IVIG acts via suppression of pathogenic immunoglobulins and B cells. Thus, whether this treatment improves CIM, which does not depend on humoral immunity for tissue injury, is of special interest. When mice with CIM were treated with high-dose IVIG (400 mg/kg) for 5 consecutive days, beginning 3 days after immunization, the incidence and histologic severity of CIM were suppressed significantly compared with that in control, saline-injected mice (Table 1).

DISCUSSION

CIM was established as a simple murine model of PM. A single injection of mice with recombinant human muscle protein induced severe and clinically significant inflammation of the skeletal muscles. CD8 T cells were enriched in the endomysial site (the site of muscle injury) as compared with their distribution in other sites of the mouse muscle. CD8 cells expressed perforins preferentially at the endomysial site. Class I MHC expression was up-regulated on the muscle fibers. Removal of CD8 T cells significantly suppressed myositis. Thus, muscle injury in CIM appears to be driven, primarily, by cytotoxic CD8 T cells, as is assumed in human PM. In this regard, the new model provides a clear contrast to the previous EAM model, which appears to be driven by CD4 T cells. Induction of EAM requires repeated immunization with a specific mouse strain having a dysferlin gene mutation that induces spontaneous muscular degeneration and inflammation. Sensitivity of B6 mice to CIM prompted the initiation of genetic studies of the pathologic mechanisms of autoimmune myositis, which would provide information for the development of new treatments.

Muscle tissues from mice with CIM contained more CD4 T cells and macrophages than are found in patients with PM, which may reflect the acute disease course of CIM. Although we observed critical participation by CD8 T cells, CD4 T cells were also important in the development of CIM. In this regard, it has been shown that the actions of CD4 T cells are essential for full differentiation of cytotoxic CD8 T cells (30,31). Alternatively, CD4 T cells may also injure muscle tissues directly. This issue should be addressed further in future experiments.

Severe inflammation was found consistently in the proximal muscles of the lower extremities, but not in other sites. Although injection of CFA alone did not induce myositis, we assume that activation of local innate immunity by injection of the foot pad with CFA would contribute to induction of severe myositis. Unlike inflammation in human PM, inflammation in other myositis models, such as EAM and cardiac myosin–induced myocarditis, is transient (32,33). Because lipopolysaccharide injection in the recovery phase of experimental myocarditis can induce a relapse of inflammation (33), unknown factors might perpetuate the chronic disease in humans.

An elevation in the levels of creatine kinase (CK) was found in the mice with CIM. However, since some mice, including healthy animals, have unexpectedly high levels of CK, this elevation could be attributed to uncontrollable hemolysis. Lung involvement in some patients is characteristic of PM and also of dermatomyositis (DM). However, no abnormality in the lungs was observed in the mice with CIM. Considering the frequency of lung disease in PM (34), we may have to undertake extensive studies of this issue using a large number of animals.

Recombinant C protein was used to confirm its immunogenicity, as suggested in a rat myositis model induced by biochemically purified C protein (19). Large-scale production of recombinant C protein fragments in the prokaryotic expression system facilitated multiple experiments to optimize an immunization protocol and to analyze the pathologic features of myositis. Since at least 200 μg of the immunogen had to be injected to induce CIM consistently, we needed to use the back and foot pads of the mice for immunization.

The rotarod test was useful to assess muscle function in the mice with CIM at a single time point. Analysis by Spearman's rank correlation coefficient showed that the rotarod score correlated well with the histologic score ($P < 0.001$). However, this test was less useful in evaluating the disease course in these mice, because the mice could learn how to run for a longer period of time when the test was repeated. We believe that the device should be improved so that muscle function or weakness can be evaluated in an easier way.

Unlike in the EAM model, many strains of mice, including SJL/J mice, were susceptible to CIM. This fact confirms the immunogenicity of the C protein and suggests that mouse strains may have their own hierarchy of susceptibility to myositis.

Our observations of CIM induced in the B6 mice with mutations in inflammatory cytokine genes demon-

strated the importance of IL-1, but not TNFα, in the development of myositis. Previous histologic studies of PM muscle tissue showed that IL-1 and other proinflammatory cytokines, including TNFα, IL-6, and interferon-γ, are expressed by mononuclear cells in the affected muscle tissue (25). IL-1 expression by mononuclear cells accompanies expression of class I MHC molecules on the muscle fibers and expression of adhesion molecules, such as intercellular adhesion molecule 1 and vascular cell adhesion molecule 1, on endothelial cells in muscle (35). Thus, we assume that IL-1 expression of activated macrophages up-regulates expression of the class I MHC molecules, as well as that of adhesion molecules and chemokines, on muscle fibers, endothelial cells, and inflammatory cells. All of these molecules can trigger CD8-mediated muscle damage. Other studies have shown that antigen-specific T cell responses are impaired in IL-1α/β double-null mutant mice (36,37). In the autoimmune myocarditis model, IL-1 is important for efficient activation of dendritic cells (DCs) and priming of CD4 T cells (38). IL-1 may also contribute to activation of DCs and interacting T lymphocytes.

Similar to IL-1, TNFα induces expression of class I MHC molecules on muscle fibers and expression of adhesion molecules on endothelial cells (39,40). The results of one report suggested that TNFα released from infiltrating CD8 T cells in PM muscles was responsible for the muscle damage (26). However, we found that CD8 T cells can induce typical myositis without TNFα. In this regard, experimental myocarditis is suppressed in both IL-1 receptor– and TNFα receptor–null mutant mice (38,41), and this model is mediated by pathogenic CD4 T cells (33,38). Thus, it is important to note the differences between the 2 murine myositis models.

Our results do not necessarily refute the idea that TNFα is a therapeutic target in PM. Clinical findings from sporadic reports suggest that some patients with PM respond to systemic delivery of anti-TNFα mAb (42). This fact and our results are similar to the findings in collagen-induced arthritis (CIA), which is an animal model of RA. TNFα-null mutant mice are susceptible to CIA (43), but inhibition of TNFα can improve the disease (9). Development of arthritis is suppressed in IL-1α/β double-null mutant mice (37). Studies are in progress to investigate the therapeutic effects of IL-1 or TNFα blockade in CIM.

A high dose of IVIGs, pooled from the plasma of healthy donors, is commonly administered as treatment in patients with autoimmune disorders (44). After an initial study showing that a patient with refractory PM was successfully treated with IVIG (29), the efficacy has been confirmed by a number of studies of patients with PM and DM (27,28). Currently, IVIG therapy is the only treatment that does not induce general immune suppression. The same treatment exerted a minor therapeutic effect in SJL/J mice in the myositis model (45). Although immunoglobulins are derived from human sera, the effect was not due to nonspecific immunomodulation by a xenogenic protein.

We found that IVIG treatment was markedly effective in CIM, suggesting its relevance as a model for human PM. When the treatment was started 8 days after immunization of the mice, the therapeutic effect appeared milder (results not shown). The mode of action of IVIGs could vary, and all of the mechanisms have not been fully characterized (46–48). Modulation of crystallizable fragment Fcγ receptor IIb on phagocytes appears to be the primary mechanism for an increase in platelet counts in patients with immune thrombocytopenia (49). Theoretically, the treatment could also down-regulate activating Fcγ receptors, increase IgG catabolism, neutralize autoantibodies and inflammatory cytokines, attenuate complement-mediated tissue damage, and modulate cytokine production by B cells and monocytes. Because development of CIM does not depend on B cells or antibodies, the efficacy of IVIG treatment for this model suggests that down-regulation of B cells or autoantibody-mediated processes are not a prerequisite to achieve improvement of PM. Further evaluation should lead to identification of key molecules for the effect of IVIG and development of new treatments that target defined molecules.

Our new model mimics human PM and provides a useful tool to investigate its pathologic mechanisms. It holds promise for identification of specific targets that will lead to the development of new therapeutic approaches in the treatment of PM, and will also be useful for confirming the efficacy of these treatments.

ACKNOWLEDGMENTS

We thank H. Karasuyama for providing the Igμ-null mutant mice, K. Sekikawa for the TNFα-null mutant mice, M. Azuma for the hybridoma-producing anti-CD8 (53.67.2) mAb, A. Suwa and T. Mimori for performing the detection of autoantibodies, and E. Hirasawa for her critical advice.

AUTHOR CONTRIBUTIONS

Dr. Kohsaka had full access to all of the data in the study and takes responsibility for the integrity of the data and the accuracy of the data analysis.

Study design. Sugihara, Kohsaka.

Acquisition of data. Sugihara, Sekine, Nakae, Kohyama.

Analysis and interpretation of data. Sugihara, Harigai, Iwakura, Matsumoto, Miyasaka, Kohsaka.
Manuscript preparation. Sugihara, Kohsaka.
Statistical analysis. Sugihara, Kohsaka.

REFERENCES

1. Dalakas MC, Hohlfeld R. Polymyositis and dermatomyositis. Lancet 2003;362:971–82.
2. Arahata K, Engel AG. Monoclonal antibody analysis of mononuclear cells in myopathies. I. Quantitation of subsets according to diagnosis and sites of accumulation and demonstration and counts of muscle fibers invaded by T cells. Ann Neurol 1984;16:193–208.
3. Engel AG, Arahata K. Monoclonal antibody analysis of mononuclear cells in myopathies. II. Phenotypes of autoinvasive cells in polymyositis and inclusion body myositis. Ann Neurol 1984;16: 209–15.
4. Goebels N, Michaelis D, Engelhardt M, Huber S, Bender A, Pongratz D, et al. Differential expression of perforin in muscle-infiltrating T cells in polymyositis and dermatomyositis. J Clin Invest 1996;97:2905–10.
5. Emslie-Smith AM, Arahata K, Engel AG. Major histocompatibility complex class I antigen expression, immunolocalization of interferon subtypes, and T cell-mediated cytotoxicity in myopathies. Hum Pathol 1989;20:224–31.
6. Bender A, Ernst N, Iglesias A, Dornmair K, Wekerle H, Hohlfeld R. T cell receptor repertoire in polymyositis: clonal expansion of autoaggressive CD8+ T cells. J Exp Med 1995;181:1863–8.
7. Nishio J, Suzuki M, Miyasaka N, Kohsaka H. Clonal biases of peripheral CD8 T cell repertoire directly reflect local inflammation in polymyositis. J Immunol 2001;167:4051–8.
8. Lipsky PE, van der Heijde DM, St.Clair EW, Furst DE, Breedveld FC, Kalden JR, et al, for the Anti–Tumor Necrosis Factor Trial in Rheumatoid Arthritis with Concomitant Therapy Study Group. Infliximab and methotrexate in the treatment of rheumatoid arthritis. N Engl J Med 2000;343:1594–602.
9. Williams RO, Feldmann M, Maini RN. Anti-tumor necrosis factor ameliorates joint disease in murine collagen-induced arthritis. Proc Natl Acad Sci U S A 1992;89:9784–8.
10. Takagi N, Mihara M, Moriya Y, Nishimoto N, Yoshizaki K, Kishimoto T, et al. Blockage of interleukin-6 receptor ameliorates joint disease in murine collagen-induced arthritis. Arthritis Rheum 1998;41:2117–21.
11. Taniguchi K, Kohsaka H, Inoue N, Terada Y, Ito H, Hirokawa K, et al. Induction of the p16INK4a senescence gene as a new therapeutic strategy for the treatment of rheumatoid arthritis. Nat Med 1999;7:760–7.
12. Rosenberg NL, Ringel SP, Kotzin BL. Experimental autoimmune myositis in SJL/J mice. Clin Exp Immunol 1987;68:117–29.
13. Matsubara S, Shima T, Takamori M. Experimental allergic myositis in SJL/J mice immunized with rabbit myosin B fraction: immunohistochemical analysis and transfer. Acta Neuropathol (Berl) 1993;85:138–44.
14. Bittner RE, Anderson LV, Burkhardt E, Bashir R, Vafiadaki E, Ivanova S, et al. Dysferlin deletion in SJL mice (SJL-Dysf) defines a natural model for limb girdle muscular dystrophy 2B. Nat Genet 1999;23:141–2.
15. Rosenberg NL, Kotzin BL. Aberrant expression of class II MHC antigens by skeletal muscle endothelial cells in experimental autoimmune myositis. J Immunol 1989;142:4289–94.
16. Weber FE, Vaughan KT, Reinach FC, Fischman DA. Complete sequence of human fast-type and slow-type muscle myosin-binding-protein C (MyBP-C): differential expression, conserved domain structure and chromosome assignment. Eur J Biochem 1993;216:661–9.
17. Gilbert R, Cohen JA, Pardo S, Basu A, Fischman DA. Identification of the A-band localization domain of myosin binding proteins C and H (MyBP-C, MyBP-H) in skeletal muscle. J Cell Sci 1999;112:69–79.
18. Kojima T, Tanuma N, Aikawa Y, Shin T, Sasaki A, Matsumoto Y. Myosin-induced autoimmune polymyositis in the rat. J Neurol Sci 1997;151:141–8.
19. Kohyama K, Matsumoto Y. C protein in the skeletal muscle induces severe autoimmune polymyositis in Lewis rats. J Neuroimmunol 1999;98:130–5.
20. Horai R, Asano M, Sudo K, Kanuka H, Suzuki M, Nishihara M, et al. Production of mice deficient in genes for interleukin (IL)-1α, IL-1β, IL-1α/β, and IL-1 receptor antagonist shows that IL-1β is crucial in turpentine-induced fever development and glucocorticoid secretion. J Exp Med 1998;187:1463–75.
21. Kubo S, Nakayama T, Matsuoka K, Yonekawa H, Karasuyama H. Long term maintenance of IgE-mediated memory in mast cells in the absence of detectable serum IgE. J Immunol 2003;170:775–80.
22. Taniguchi T, Takata M, Ikeda A, Momotani E, Sekikawa K. Failure of germinal center formation and impairment of response to endotoxin in tumor necrosis factor α-deficient mice. Lab Invest 1997;77:647–58.
23. Moll J, Barzaghi P, Lin S, Bezakova G, Lochmuller H, Engvall E, et al. An agrin minigene rescues dystrophic symptoms in a mouse model for congenital muscular dystrophy. Nature 2001;413:302–7.
24. Mogi S, Sakurai J, Kohsaka T, Enomoto S, Yagita H, Okumura K, et al. Tumour rejection by gene transfer of 4-1BB ligand into a CD80+ murine squamous cell carcinoma and the requirements of co-stimulatory molecules on tumour and host cells. Immunology 2000;101:541–7.
25. Lundberg I, Ulfgren AK, Nyberg P, Andersson U, Klareskog L. Cytokine production in muscle tissue of patients with idiopathic inflammatory myopathies. Arthritis Rheum 1997;40:865–74.
26. Kuru S, Inukai A, Liang Y, Doyu M, Takano A, Sobue G. Tumor necrosis factor-α expression in muscles of polymyositis and dermatomyositis. Acta Neuropathol (Berl) 2000;99:585–8.
27. Cherin P, Pelletier S, Teixeira A, Laforet P, Genereau T, Simon A, et al. Results and long-term followup of intravenous immunoglobulin infusions in chronic, refractory polymyositis: an open study with thirty-five adult patients. Arthritis Rheum 2002;46:467–74.
28. Dalakas MC, Illa I, Dambrosia JM, Soueidan SA, Stein DP, Otero C, et al. A controlled trial of high-dose intravenous immune globulin infusions as treatment for dermatomyositis. N Engl J Med 1993;329:1993–2000.
29. Cherin P, Herson S, Wechsler B, Piette JC, Bletry O, Coutellier A, et al. Efficacy of intravenous gammaglobulin therapy in chronic refractory polymyositis and dermatomyositis: an open study with 20 adult patients. Am J Med 1991;91:162–8.
30. Sun D, Whitaker JN, Huang Z, Liu D, Coleclough C, Wekerle H, et al. Myelin antigen-specific CD8+ T cells are encephalitogenic and produce severe disease in C57BL/6 mice. J Immunol 2001; 166:7579–87.
31. Edith M, Janssen EE, Lemmens TW, Urs C, Matthias GH, Stephen PS. CD4+ T cells are required for secondary expansion and memory in CD8+ T lymphocytes. Nature 2003;421:852–6.
32. Matsubara S, Kitaguchi T, Kawata A, Miyamoto K, Yagi H, Hirai S. Experimental allergic myositis in SJL/J mouse: reappraisal of immune reaction based on changes after single immunization. J Neuroimmunol 2001;119:223–30.
33. Eriksson U, Ricci R, Hunziker L, Kurrer MO, Oudit GY, Watts TH, et al. Dendritic cell-induced autoimmune heart failure requires cooperation between adaptive and innate immunity. Nat Med 2003;9:1484–90.
34. Marie I, Hachulla E, Cherin P, Dominique S, Hatron PY, Hellot MF, et al. Interstitial lung disease in polymyositis and dermatomyositis. Arthritis Rheum 2002;47:614–22.
35. Lundberg I, Kratz AK, Alexanderson H, Patarroyo M. Decreased expression of interleukin-1α, interleukin-1β, and cell adhesion

molecules in muscle tissue following corticosteroid treatment in patients with polymyositis and dermatomyositis. Arthritis Rheum 2000;43:336–48.
36. Nakae S, Asano M, Horai R, Sakaguchi N, Iwakura Y. IL-1 enhances T cell-dependent antibody production through induction of CD40 ligand and OX40 on T cells. J Immunol 2001;167:90–7.
37. Saijo S, Asano M, Horai R, Yamamoto H, Iwakura Y. Suppression of autoimmune arthritis in interleukin-1–deficient mice in which T cell activation is impaired due to low levels of CD40 ligand and OX40 expression on T cells. Arthritis Rheum 2002;46:533–44.
38. Eriksson U, Kurrer MO, Sonderegger I, Iezzi G, Tafuri A, Hunziker L, et al. Activation of dendritic cells through the interleukin 1 receptor 1 is critical for the induction of autoimmune myocarditis. J Exp Med 2003;197:323–31.
39. Nagaraju K, Raben N, Merritt G, Loeffler L, Kirk K, Plotz P. A variety of cytokines and immunologically relevant surface molecules are expressed by normal human skeletal muscle cells under proinflammatory stimuli. Clin Exp Immunol 1998;113:407–14.
40. Mantovani A, Bussolino F, Dejana E. Cytokine regulation of endothelial cell function. FASEB J 1992;6:2591–9.
41. Wada H, Saito K, Kanda T, Kobayashi I, Fujii H, Fujigaki S, et al. Tumor necrosis factor-α (TNF-α) plays a protective role in acute viral myocarditis in mice: a study using mice lacking TNF-α. Circulation 2001;103:743–9.
42. Anandacoomarasamy A, Howe G, Manolios N. Advanced refractory polymyositis responding to infliximab. Rheumatology (Oxford) 2005;44:562–3.
43. Campbell IK, O'Donnell K, Lawlor KE, Wicks IP. Severe inflammatory arthritis and lymphadenopathy in the absence of TNF. J Clin Invest 2001;107:1519–27.
44. Sapir T, Blank M, Shoenfeld Y. Immunomodulatory effects of intravenous immunoglobulins as a treatment for autoimmune diseases, cancer, and recurrent pregnancy loss. Ann N Y Acad Sci 2005;1051:743–78.
45. Wada J, Shintani N, Kikutani K, Nakae T, Yamauchi T, Takechi K. Intravenous immunoglobulin prevents experimental autoimmune myositis in SJL mice by reducing anti-myosin antibody and by blocking complement deposition. Clin Exp Immunol 2001; 124:282–9.
46. De Grandmont MJ, Racine C, Roy A, Lemieux R, Neron S. Intravenous immunoglobulins induce the in vitro differentiation of human B lymphocytes and the secretion of IgG. Blood 2003;101: 3065–73.
47. Basta M, Dalakas MC. High-dose intravenous immunoglobulin exerts its beneficial effect in patients with dermatomyositis by blocking endomysial deposition of activated complement fragments. J Clin Invest 1994;94:1729–35.
48. Kaveri S, Vassilev T, Hurez V, Lengagne R, Lefranc C, Cot S, et al. Antibodies to a conserved region of HLA class I molecules, capable of modulating CD8 T cell-mediated function, are present in pooled normal immunoglobulin for therapeutic use. J Clin Invest 1996;97:865–9.
49. Samuelsson A, Towers TL, Ravetch JV. Anti-inflammatory activity of IVIG mediated through the inhibitory Fc receptor. Science 2001;291:484–6.

Available online at www.sciencedirect.com
ScienceDirect
Neuroscience Research 59 (2007) 457–466
Neuroscience Research
www.elsevier.com/locate/neures

Inhibition of glial cell activation ameliorates the severity of experimental autoimmune encephalomyelitis

Xiaoli Guo [a], Kazuaki Nakamura [a], Kuniko Kohyama [b], Chikako Harada [a], Heather A. Behanna [c], D. Martin Watterson [c], Yoh Matsumoto [b], Takayuki Harada [a,*]

[a] Department of Molecular Neurobiology, Tokyo Metropolitan Institute for Neuroscience, 2-6 Musashidai, Fuchu, Tokyo 183-8526, Japan
[b] Department of Molecular Neuropathology, Tokyo Metropolitan Institute for Neuroscience, 2-6 Musashidai, Fuchu, Tokyo 183-8526, Japan
[c] Center for Drug Discovery and Chemical Biology, Northwestern University, Chicago, IL 60611, USA

Received 8 May 2007; accepted 23 August 2007
Available online 30 August 2007

Abstract

Activated microglia and astrocytes have been implicated in the course of multiple sclerosis (MS) and its animal model: experimental autoimmune encephalomyelitis (EAE). MW01-5-188WH is a novel drug that selectively inhibits glial activation in the central nervous system (CNS). We report here that MW01-5-188WH is effective to ameliorate the severity of myelin oligodendrocyte glycoprotein (MOG)-induced EAE. Daily oral administration of MW01-5-188WH at 5 mg/kg body weight reduced the clinical scores of EAE mice while having no influence on the disease incidence or animal mortality. Pathological examination revealed reduced numbers of microglia and astrocytes in the spinal cord of MW01-5-188WH-treated EAE mice. Moreover, MW01-5-188WH suppressed the release of key chemokines, which are involved in MS pathology, from cultured microglia and astrocytes. Taken together, our results indicate that treatments that suppress the activation of microglia and astrocytes should be pursued in future research for their potential as avenues for the treatment of MS.

Keywords: Astrocytes; Chemokines; Experimental autoimmune encephalomyelitis; Glial activation; Microglia; Mouse; MW01-5-188WH; Spinal cord

1. Introduction

Multiple sclerosis (MS) and its animal model, experimental autoimmune encephalomyelitis (EAE), are inflammatory diseases of the central nervous system (CNS) characterized by localized areas of demyelination. The current pathophysiological concept of MS includes genetic and environmental factors as well as a dysfunction in immune regulation. Recent studies have shown the importance of the local environment, especially the activation of glial cells during MS (Ponomarev et al., 2005; Tanuma et al., 2006; Farina et al., 2007). For example, in the gray matter of spinal cord in EAE mice, there are activated astrocytes with increased expression of glial fibrillary acidic protein (GFAP; Liedtke et al., 1998) and activated microglia with increased expression of membrane attack complex-1 (Mac-1; Aharoni et al., 2005). These activated glia produce nitric oxide (NO), proinflammatory cytokines [interferon-γ (IFN-γ), tumor necrosis factor-α (TNF-α), etc.] and chemokines that may contribute to disease progression and related oligodendrocyte cell death (Hisahara et al., 2001; Tanuma et al., 2006; Xu and Drew, 2006). Several chemokines regulated on activation, such as normal T cell expressed and secreted proteins (RANTES), interferon-γ-inducible protein of 10 kDa (IP-10) and monocyte chemoattractant protein (MCP-1), are reported to be upregulated in both MS (Balashov et al., 1999; Van Der Voorn et al., 1999) and EAE (Godiska et al., 1995; Glabinski et al., 1997; Juedes et al., 2000). Consistently, these key chemokines have been linked to the clinical severity of MS and EAE (Godiska et al., 1995; Glabinski et al., 1997; Karpus and Kennedy, 1997; Miyagishi et al., 1997; Balashov et al., 1999; Van Der Voorn et al., 1999; Juedes et al., 2000). Thus, chemokine production can be used as a marker for microglia/astrocyte activation during MS or EAE.

MW01-5-188WH, an orally bioavailable and brain-penetrating small molecule compound that is a novel CNS experimental therapeutic that targets glial activation (Ralay Ranaivo et al., 2006). MW01-5-188WH suppressed the

* Corresponding author. Tel.: +81 42 325 3881; fax: +81 42 321 8678.
E-mail address: harada@tmin.ac.jp (T. Harada).

0168-0102/$ – see front matter
doi:10.1016/j.neures.2007.08.014